



**UNIVERSITA' DEGLI STUDI DI TORINO**

*Department of Oncological Sciences*

**Ph.D. in Complex Systems applied to Post-Genomic Biology**

XXIII Cycle

**miR-148b is a major coordinator in a Relapse-associated  
miR signature in Breast Tumors**

**Cimino Daniela**

*Supervisor:* **Prof.ssa Daniela Taverna**

*Tutor:* **Prof. Michele De Bortoli**

*Coordinator:* **Prof. Michele Caselle**

SSD: BIO/11  
ACADEMIC YEARS: 2008/2010

# INDEX

<b>ABSTRACT</b> .....	3
<b>INTRODUCTION</b> .....	6
<b>RESULTS</b> .....	13
A 16 miRNA signature associates with survival and shows a significant classification power.....	14
miR-148b coordinates many signal transduction pathways .....	15
miR-148b influences cell growth, adhesion and invasion.....	16
miR-148b expression enhances chemotherapy-induced apoptosis.....	17
miR-148b modulates multiple genes.....	18
The miR-148b host gene, COPZ1, is associated with survival .....	20
miR-148b is part of a Feed Forward Loop (FFL) .....	20
<b>FIGURES</b> .....	22
<b>TABLES</b> .....	61
<b>MATERIALS AND METHODS</b> .....	70
<b>DISCUSSION</b> .....	84
<b>ACKNOWLEDGEMENTS</b> .....	91
<b>BIBLIOGRAPHY</b> .....	92
<b>REVIEWER COMMENTS</b> .....	97

# ABSTRACT

Cancer is a multistep disease controlled by a wide spectrum of genetic and epigenetic changes occurring within a cell as well as environmental influences. Cell transitions are often investigated as single gene mutation/expression modulations however it is essential to evaluate the molecular context in which the altered genes operate and how various changes are connected with each other referring to *gene networks*. Cell alterations have been mostly related to protein-coding genes however it is now essential to investigate the role of non-coding genes, such as microRNAs (miRNAs), since they seem to be highly involved in tumor progression.

miRNAs are small non-coding RNAs frequently altered in human malignancies. They regulate protein-coding gene expression by mediating mRNA degradation and/or repressing translation via the association with the 3' untranslated region (3' UTR) of the mRNAs. Aberrant miRNA expression can influence several gene networks and pathways implicated in tumorigenesis and metastasis formation.

To reveal miRNAs involved in breast cancer progression we investigated miRNA expression in 77 ductal breast carcinoma biopsies and 17 mammoplasties by microarray analysis. 16 differentially expressed miRNAs were identified comparing patients with or without disease relapse within 72 months from surgery.

In my project, I evaluated the relevance of the 16 miRNA relapse-signature to predict survival and identified the signalling pathways in which they were involved. In addition, I assessed how one of the small RNAs present in this signature, miR-148b, was able to coordinate tumorigenesis and identified some of its biological targets.

Putative miRNA target analysis for the relapse-signature miRNAs was performed employing miRecords and 14,535 potential targets were found. When Ingenuity Pathway Analysis systems (IPA) were applied to the entire set of targets, a significant and specific

enrichment in 62 cancer related pathways was found, examples are integrins, mTOR, PI3K/AKT and ERK/MAP signaling pathways. Among the 16 deregulated miRNAs, miR-148b was predicted to control a great percentage (25%) of the putative targets and to coordinate the highest number of pathways; therefore we studied its biological relevance in details. When expression of miR-148b was modulated (up- or down-regulation) in breast cancer, *in vitro* cell growth, adhesion, anoikis, invasion as well as chemotherapy-induced apoptosis were altered. To identify which miR-148b targets were involved in tumorigenesis, a microarray analysis was performed for miR-148b over-expressing cells versus controls and 129 (49 up and 80 down) modulated genes were revealed. 33 of these 129 genes were predicted targets as well. Among them, ITGA5 was found to be down-modulated at the protein level via a direct binding of miR-148b on its 3' UTR. Since various downstream effectors of integrins were miR-148b predicted targets, we investigated the integrin signalling and proved that ROCK1, p110 $\alpha$  (PIK3CA) and NRAS were regulated by miR-148b suggesting a multiple control of the integrin pathway by miR-148b.

In parallel, we identified a specific regulatory Feed Forward Loop (FFL) that involves ITGA5, miR-148b and the transcription factor, c-REL that we are now investigating.

Our findings underline the relevance of the identified relapse-signature for patient prognosis and show that miR-148b is able to regulate gene networks that coordinate breast cancer progression and the response to chemotherapy.

# INTRODUCTION

Despite the efforts to improve survival and reduce mortality rates, breast cancer still remains the most common malignancy for women in the world (1). The main cause of death for breast cancer patients is due to complications arising from metastasis (1, 2).

Many clinical and pathological evidences are routinely used to categorize patients with breast cancer in order to assess prognosis and to determine the appropriate therapy. These “read out” are morphological characteristics and include tumor size, lymph node involvement, histological grade and age (3). Unfortunately this approach is not accurate enough and leads to a high number of over or poorly-treated patients. In particular the main concern in clinics is related to lymph node negative breast cancer (LN-); it is known that only the 20–30% of these patients die from recurrent disease (4). Due to that two-third of LN- patients could be spared chemotherapy, but no way to identify them was presented to date. On the other side, lymph node positive patients could be classified for tailored treatments, on the basis of other biological markers.

The use of tumor molecular markers significantly enhances the ability to stratify patients according to risks and better allows the appropriate therapy tailoring. Estrogen receptor (ER) and progesterone receptor (PR) status are validated prognostic molecular markers. Estrogen receptor expression also predicts for response to hormone therapy such as tamoxifen or aromatase inhibitors (5). On the other hand, chemotherapy seems to be more beneficial for patients with ER-negative tumors (6). Based on these findings, patients with small tumors and elevated ER expression with a low risk of disease recurrence may be spared the toxicity of adjuvant chemotherapy and treated with hormone therapy alone in the adjuvant setting. The challenge is how to identify these tumors in the best way. The HER2 gene (ErbB2, commonly referred to as HER2/*neu*) is a newer biological marker routinely tested in all breast cancer tumors (7). HER2 is a 185-kD transmembrane protein with intrinsic

tyrosine kinase activity that has a role in cell growth regulation (8). It is amplified in 17%-30% of breast cancer tumors and is associated with poor prognosis (9). The addition of agents that specifically target HER2 to adjuvant chemotherapy regimens has significantly improved the survival of patients with HER2-positive (HER2+) disease and has altered the natural history of this subtype of breast cancer (10).

The combination of morphological and molecular markers gives better clinical results than the use of each approach alone. The combination of these two methodologies has been applied to groups of patients in various ways and led to the formation of various risk categories such as the St Gallen criteria (11), the NIH consensus criteria (12), the Nottingham Prognostic Index (13), and Adjuvant!Online ([www.adjuvantonline.com](http://www.adjuvantonline.com)). Although these factors have been useful to assess prognosis and risk in groups of patients, their role for individual patient with breast cancer is more limited, as patients with similar combinations of features may have very different clinical outcomes.

In recent years, gene expression profilings have been used to improve breast cancer classification and to assess prognosis and response to therapy. With this approach major breast cancer subtypes have been identified; in particular, the luminal A and luminal B groups, among the hormone receptor-positive breast cancers and the HER2+ and basal-like groups among the hormone receptor-negative tumors. Specific clinical features, responses to treatment and prognosis have been observed to correspond to the various subgroups reinforcing the power of gene expression patterns (14). The expression of certain gene sets, defined as “signatures” has been reported to be prognostic and/or predictive for patients with breast cancer (15). It is of interest to note that despite similar prognostic or predictive value, there is very little, if any, overlap in the genes included in these profiles (16).

At the moment, two molecular tests available for breast cancer patients, OncotypeDX (Genomic Health) and MammaPrint (Agendia), are based on gene expression profiles studies and deserve specific comments. OncotypeDX is a qRT-PCR-based assay that can be performed on formalin-fixed tissue from tumor paraffin blocks. It analyzes gene expression for 21 genes and provides a 'recurrence score' that correlates with outcome, likelihood of response to endocrine therapy and to chemotherapy (17, 18). Instead, MammaPrint analyzes by a specific microarray platform the expression of 70 genes to identify patients with good and poor prognostic signatures (19, 20). Both of these tests are already being used in patient management and their ultimate value will be determined by the results of prospective clinical trials that are currently underway: the TAILORx and the MINDACT trials, respectively for OncotypeDX (18) and for MammaPrint (20).

However, even if gene expression profiles have provided new biomarkers with potential use for diagnosis, drug development, and tailored therapy, they have not exhaustively elucidated all the detailed mechanisms at tumour origin and progression.

More recently new players have been found to be involved in tumorigenesis: microRNAs (miRNAs), a small class of non-coding RNAs able to regulate gene expression at post-transcriptional level, by binding at the 3' untranslated region (3' UTR) of target mRNAs and causing a block of translation and/or mRNA degradation (21). Transcription of miRNAs is typically performed by RNA polymerase II, and transcripts are capped and polyadenylated (22). miRNAs undergo two cleavage steps of maturation: one in the nucleus by the RNase DROSHA and the other one in the cytoplasm by the ribonuclease DICER. The mature miRNA duplex is a short-lived entity; it is rapidly unwound when it associates with an Ago protein into the RNA-induced silencing complex (RISC) complex. miRNA unwinding is accompanied by differential strand retention; one strand is retained while the other strand is lost (23). In the

RISC a miRNA acts as an adaptor to specifically recognize a particular mRNAs and to mediate its silencing by targeting its 3' UTR. Target mRNAs are recognized in specific target sites by partial sequence similarity in the seed sequence of the mature miRNA, generally the nucleotides 2–7 of the miRNA, which are very conserved throughout evolution. Once the target mRNA is recognized by the miR-RISC complex, it is unclear what mechanisms mediate mRNA repression: mRNA degradation in the P-bodies or inhibition of translation by blocking ribosomes (24).

Importantly, a single miRNA can influence the expression of hundreds of proteins and some miRNAs can trigger feedforward or feedback loops of gene expression regulation by synergistic cooperation with their target genes (22). Furthermore, miRNAs are found to be involved, together with transcription factors (TF), in important gene expression regulatory circuits, such as the Feed-forward loops (FFLs) (25). These elementary circuits of gene regulation are termed “mixed” feed-forward loops, involving both transcriptional (T) and posttranscriptional (PT) regulators. In particular, in these network motifs, a TF regulates an miRNA and together with it a set of Joint Target protein-coding genes. Mixed FFLs are generally identified bioinformatically and generally validated biologically. A particular database, CircuitsDB, has been recently published and used to predict mixed miRNA/TF FFLs (26). These findings reveal complex gene expression regulatory networks able to determine cellular behaviour as a whole.

Because of the high impact of miRNAs on protein-coding gene expression, not surprisingly, alteration of miRNAs has been linked to human diseases and associated, in particular, with many of the classical hallmarks of cancer, including defects in proliferation, differentiation and apoptosis. The early studies on miRNA expression profiles in tumors demonstrated that aberrant expression occurs often in tumors and it is a function of either

deletions associated with fragile sites or genomic amplification. Studies on altered miRNA expression suggest that they may be critical biomarkers of cancer (21).

The first reports describing the existence of a miRNA signature characterising human breast cancer were published in 2005 (27). The authors reported that miRNA expression, globally down-regulated in tumours in comparison with normal tissues, classifies human cancers more accurately than mRNA expression profiles, according to developmental lineage and differentiation status. In another study, it was shown that breast cancers could be classified into specific tumor pathological phenotypes (ER and PR status, proliferation, tumor stage, metastatic state, HER2 status) as well as subtypes (Luminal A, Luminal B, Basal-like, HER2+ and Normal-like) based on their miRNA expression profiles (28). Thus, miRNAs may provide additional information for the prognosis and treatment of cancer when combined with protein-coding gene expression profiling.

Accumulating data have proven that miRNAs also affect the multiple steps of the metastatic cascade by influencing cancer cell adherence, migration, invasion, motility, and angiogenesis (29). miRNAs associated with the metastatic process have recently been termed “metastamirs” and exert important roles in modulating key signalling pathways involved in metastasis, such as the NFkB, EGFR, TWIST or HIF1 $\alpha$ -induced pathways (30).

Experimental studies with xenografts in mice demonstrated that the metastatic potential of breast cancer cells could be effectively impaired by the expression of metastasis suppressor miRNAs or the neutralization of metastasis activator miRNAs, implying the feasibility of the therapeutic strategy; however, miRNAs have also promiscuous downstream targets that influence signalling events, most probably in a context dependent manner. For this reason, it is difficult to identify ideal target molecules (31).

To investigate the relationships between altered miRNA expression and breast cancer metastasis and to provide new information on the related regulatory network as a whole, we analyzed miRNA expression in a cohort of breast cancer patients, divided according to relapse onsets. We identified 16 differentially expressed miRNAs between relapsing and non-relapsing samples that showed a significant classification power also in another dataset. Among those miRNAs, miR-148b revealed functions and pathway associations common to the entire “miRNA signature” and showed significant prognostic and predictive ability when we analyzed its biological impact in details.

# RESULTS

## **A 16 miRNA signature associates with survival and shows a significant classification power**

To correlate miR expression deregulation with breast cancer progression, we analyzed miR expression in 77 human breast tumors and 17 normal tissues from mammoplastic reductions by microarrays (Human Agilent platform-V2). Only ductal carcinomas were included in our investigation: detailed information about the clinical samples is provided in the Supplementary material, Table 1. 237 out of 723 analyzed miRs were expressed in at least 60% of our samples. Two-classes SAM analysis was applied to compare miR expression in different groups of tumors defined by clinico-pathological data such as relapse onset, lymph node status and steroid receptor status. Several lists of differentially expressed miRs were obtained. By comparing miR expression in primary tumors from patients with (R+) or without (R-) disease relapse, within 72 months from surgery, considering a 16% false discovery rate (FDR), 16 differentially expressed miRs were identified (miR signature). An unsupervised hierarchical cluster of the 16 miR signature is shown in Figure 1A and the fold changes of each miR in R+ (n=41) *versus* R- (n=36) groups of tumors are provided in Figure 2 together with the expression level relative to normal breast tissue median expression from 17 mammoplastic reduction samples (log 2 of tumor sample versus control). When we investigated the link of the 16 miR signature with survival we found a significant association with both overall (P value = 0.018) and disease free survival (P value = 0.016) as shown in Figure 1B. We also observed that this correlation was independent from lymph-node (LN) status (P value = 0.015), with a Hazard Ratio (HR) of 2.7 (Confidence Interval, C.I.: 1.2-5.9) higher than the LN HR equal to 0.2 (C.I.: 0.1-0.6). Differentially expressed miRs were also found when Estrogen receptor (ER) or Progesterone Receptor (PR) or LN positive (+) or negative (-) primary tumors were compared considering a FDR of 14% or 9.3% or 7.6%

respectively. As presented in Figure 3, 4 and 5, 29 miRs were modulated between ER+ and ER- samples while 56 discriminated PR+ versus PR- and 24 separated LN+ versus LN- breast tumors. Microarray results were validated by performing qRT-PCRs for miR-148b, miR-365, miR-10a, miR-19a and miR-342 for 5 or 10 R+/R- or LN+/LN- or ER+/ER- samples and results are shown in Figure 6B (comparison with arrays, Figure 6A). The classification power of the Relapse-associated 16 miRs was investigated to predict good or bad prognosis within our group of samples (N=77) and in Blenkiron et al. dataset (N=80) (28) compared with LN status (see materials and methods). As shown in table 2 the 16 miR-signature performed better than LN status to identify good prognosis samples in our study (88% versus 72%) and in Blenkiron et al. dataset (76% versus 85%). Instead LN status performed better in sorting poor prognosis samples for both datasets (Table 2). For Blenkiron et al. samples we should underline that only 7 out of our 16 miRs were present: miR-101, miR-10a, miR-148b, miR-197, miR-142-5p, miR-374 and miR-342. Therefore the classification power refers to them.

### **miR-148b coordinates many signal transduction pathways**

To identify the biological functions coordinated by the 16 Relapse-associated miRs we looked for their potential target genes using the miRecords System (<http://mirecords.biolead.org>; at least three algorithms) and identified 14,535 predicted genes. This group of protein-coding genes was used to perform an Ingenuity Pathway Analysis (IPA) and a significant enrichment (Fisher test, p value <0.05) was found for pathways linked to tumorigenesis and cancer aggressiveness, such as integrins, mTOR, PI3K/AKT and ERK/MAP signaling pathways (Figure 7A). To assess the contribution of each miR to the various pathways we estimated the percentage of genes targeted by each miR. As shown in Table 3, miR-765 and miR-148b targeted the highest number of genes, respectively 38.1% and 25.1%. When we searched for

pathway enrichment we observed that miR-148b coordinated the higher number of pathways identified for the 16-miR signature (84 pathways out of 122 significantly enriched), moreover it showed specific overlap considering pathways related to tumorigenesis and cancer aggressiveness, for instance the integrin pathway (Figure 7B). miR-765 instead controlled 69 pathways out of the 122 related to the 16-miR signature with a lower enrichment p-value in tumor related pathways than miR-148b (data not shown). miR-148b in addition resulted modulated also in ER+/ER- and PR+/- (Figure 3 and 4). Moreover when we evaluated its correlation with survival in R+ versus R- patients a significant association with both overall (P value = 0.027) and disease free survival (P value = 0.036) was found considering high (n=44) versus low (n=33) expression tumors as shown in Figure 1D, E; this suggests its relevance in breast cancer progression. These findings, together with the fact that miR-148b expression can predict survival by itself (Figure 1D-E), brought us to investigate miR-148b biological properties in more detail.

### **miR-148b influences cell growth, adhesion and invasion**

To investigate the biological role of miR-148b, we first analyzed miR-148b expression in several mammary epithelial cell lines (human and mouse) by qRT-PCR. Low miR-148b expression was found in the human SKBR3, MDAMB468, MDAMB231 cell lines and in the mouse 4T1 mammary tumor cells (Figure 8A). Instead, intermediate or high levels of expression were identified in HBL100, MCF10A and MCF12A human normal breast cell lines, in MCF7, T47D, MDAMB435, MDAMB453, BT474 human tumor cells and in 66cl4 mouse tumor cells (Figure 8A). Second, we overexpressed miR-148b in the highly metastatic, low miR-148b expressing, MDAMB231 or in 4T1 cells in a transient manner. Alternatively we down-modulated miR-148b in MCF7 cells. Cells were transfected with miR-148b precursors or

anti-miR-148b inhibitors or negative controls (pre-miR-148b, anti-miR-148b, or control or anti-control) and miR-148b expression was measured by qRT-PCR (Figures 8B, 9A, 10A). 72h post-transfections miR-148b expression was increased up to 70-80 folds in pre-miR-148b-transfected MDAMB231 or 4T1 cells (Figure 8B) or 50% decreased in anti-miR-148b-transfected MCF7 cells (Figure 10A). When cell proliferation in plates was analyzed for overexpressing MDAMB213 cells, we observed increased cell number up to 4 days, in presence of miR-148b transient overexpression compared with negative controls (Figure 11A). In parallel acceleration of cell cycle was found with 10% increase in G2/M phase cells (Figure 11B). Instead anchorage-independent growth in soft agar was reduced, since the number and the size of colonies for transiently miR-148b overexpressing MDAMB231 cells were lower than controls (Figure 11C).

When we looked for miR-148b involvement in cell adhesion, we observed significant adhesion alterations on different extracellular matrices (ECMs). In particular, transient miR-148b overexpression in MDAMB231 cells improved adhesion on fibronectin (FN), laminin (LN) and collagen IV (COL IV, 0.5-2-fold increase) (Figures 11D). Conversely, downmodulation of miR-148b in MCF7 cells led to decreased adhesion on FN and COL IV (Figure 10B); MCF7 cells didn't stick on LN. Significantly, miR-148b overexpression by pre-miR-148b transfection in MDAMB231 (figure 11E) or 4T1 (Figure 9) cells reduced cell invasion through fibronectin or matrigel respectively as evaluated by transwell assays compared with negative controls. Instead we didn't observe any significant difference in migration (data not shown).

### **miR-148b expression enhances chemotherapy-induced apoptosis**

To evaluate miR-148b effects in cell survival processes, MDAMB231 cell were transfected with miR-148b precursors or negative controls (pre-miR-148b or control), treated with

Staurosporine (STS) or Paclitaxel (PTX) or Cis-platin (CDDP) or Doxorubicine (DOXO) or left untreated (basal) for 48h and analyzed for cell death by AnnexinV-FITC/TMRM staining and cytofluorimetric analyses (Figure 12 and 13). In average, 15% reduction in cell survival was observed for miR-148b overexpressing cells versus controls following STS treatment (Figure 13), while 8%, 10% and 11% decrease was respectively found for PTX, CDDP and DOXO-treated cells (Figure 12A), all compared with basal samples. When we evaluated apoptosis in absence of adhesion (anoikis) and serum for 72h for the same cells an averaged 15% reduction in cell survival was identified in miR-148 overexpressing cells versus controls (Figure 12B).

### **miR-148b modulates multiple genes**

The effects of miR-148b on cancer progression depend on the direct and indirect regulation of multiple target genes. To identify miR-148b modulated genes, MDAMB231 cells were transfected with miR-148b precursors or negative controls (pre-miR-148b or control) and used 48h or 72h later for microarray and western blot (WB) analyses. When a “Whole Human Genome Oligo Microarray” (Agilent) platform was employed, 129 differentially expressed genes (49 upregulated, 80 downmodulated) were found at 48h, considering a fold change (FC) cut of 1.5 and a false discovery rate (FDR) of 16% (Table 4). Validation of the microarray analysis was performed by qRT-PCR assays as shown in Figure 14. Crossing these results with the list of putative miR-148b targets (3642) obtained by the miRecords System, we observed that 33 of the modulated genes were also miR-148b predicted targets and interestingly, 26 out of these 33 genes were downmodulated, as shown in Figure 15A in a heatmap clustering image. When we looked at the specific contribution of these 33 genes in the enriched pathways identified by IPA analysis, 11 genes (PDIA3, CSF1, NRP1, ITGA5,

RTN4 and MMP15 downmodulated; BCL2, GNA13, CDK6, RPS6KB1 and FZD5 upregulated) were part of cancer related pathways such as Integrin, Apoptosis and ERK/MAP Signalings (data not shown). Considering the involvement of ITGA5 in apoptosis, adhesion, migration/invasion we investigated the possible direct regulation of ITGA5 by miR-148b and the involvement of this regulation in tumor progression. Since ROCK1, p110 $\alpha$  (PI3KCA) and NRAS are well known downstream effectors of integrins, identified as potential miR-148b targets by miRecords (see IPA integrin signaling in Figure 16), we studied the possible functional link between these genes and miR-148b as well. Protein expression of ITGA5, ROCK1, p110 $\alpha$  (PI3KCA) and NRAS resulted diminished (from 17% to 48% repression) in miR-148b overexpressing MDAMB231 cells 48h or 72h post-transfection, compared with negative controls, as measured by WB analysis (Figure 15B). Normalization was performed against the heat shock protein 90 (hsp90), as shown in Figure 15B. However only ITGA5 but not ROCK1, p110 $\alpha$  (PI3KCA) and NRAS were modulated at the mRNA level as seen by microarray analysis and qRT-PCR validations (Figure 14). To assess a direct modulation of miR-148b on these genes, we performed specific reporter assays. The 3'UTRs of ITGA5, ROCK1 and p110 $\alpha$  (PI3KCA) were cloned into a reporter vector and Luciferase assays performed in MDAMB231 cells transfected with miR-148b precursors or negative controls (pre-miR-148b or control). As shown in Figure 15C, Luciferase expression driven by the 3'UTRs of ITGA5, ROCK1 and p110 $\alpha$  (PI3KCA) was significantly repressed. As a positive control, a miR-148b-sensor construct, containing 3 perfect bindings for miR-148b, was used for each experiment (Figures 15C). To investigate if the ITGA5 Luciferase expression regulation depended on the binding between miR-148b seed and the complementary a and b sequences present on the 3'UTRs of ITGA5, a 3 point mutations were inserted in a and b in the ITGA5 3'UTR, as indicated in Figure 15D/E. These 3'UTR alterations completely

abrogated the effect of miR-148b overexpression on Luciferase expression in MDAMB231 cells (Figure 15E), indicating a specific and direct regulation of miR-148b on ITGA5 3'UTR binding sites.

### **The miR-148b host gene, COPZ1, is associated with survival**

As shown in Figure 17A miR-148b is located in the first intron of the COPZ1 gene (Chromosome 12: 54,718,911-54,745,633 forward strand). To assess the relevance of COPZ1 in breast cancer progression and its relation with miR-148b we measured the expression of COPZ1 in our breast cancer samples by qRT-PCR and looked for an association with survival. COPZ1 expression associated significantly with both overall and disease free survival, as for miR-148b (Figure 17B). Moreover, COPZ1 expression showed a significant positive correlation with miR-148b expression (Spearman Rho correlation coefficient = 0.5, two tail P value < 0.001).

### **miR-148b is part of a Feed Forward Loop (FFL)**

To assess if miR-148b is an important player in transcriptional regulatory networks we explored CircuitsDB, a database of over-represented regulatory circuits in which a Transcription Factor regulates a miR and together with it a set of Joint Target protein-coding genes (Mixed Feed Forward Loop, FFL) (<http://biocluster.di.unito.it/circuits/>) (26). Interestingly 22 out of 148 miR-148b related circuits linked miR-148b to c-REL, a member of the NFkB family. c-REL in miR-148b selected circuits was the overrepresented Transcription Factor. Moreover among the miR-148b/c-REL joint targets we found ITGA5. To investigate the relationship between c-REL and miR-148b we silenced c-REL in MCF7 cells and we analyzed miR-148b and ITGA5 expression modulations. ITGA5 protein expression resulted diminished

(from 33% to 25% repression) in MCF7/c-REL silenced cells 48h or 72h post-transfection, compared with negative controls, as measured by WB analysis (Figure 18A). miR-148b expression instead was upregulated by c-REL downmodulation in MCF7/c-REL silenced cells 48h or 72h post-transfection, compared with negative controls; qRT-PCR measurement showed in a representative experiment an increase in miR-148b expression of 1.5 fold at 48h post-transfection and of 2.5 fold at 72h post-transfection (Figure 18A). These experimental evidences validated the miR-148b-ITGA5-c-REL regulatory circuit; to understand the function of this particular FFL it is necessary to investigate c-REL/ITGA5 relationship.

# FIGURES

**Figure 1 – Expression of the 16 most modulated miRs comparing tumor samples with or without relapse and association with overall or disease free survival. (A)** Unsupervised two-dimensional hierarchical clustering (Pearson correlation, average linkage) for the 16 most modulated miRs considering relapse (n=41) versus non-relapse (n=36) tumors. Heatmap colors represent relative miR expression referring to the median expression of miRs across all samples, as indicated in the color key panel, median: black; row: miR; column: tumor sample. **(B, C, D, E)** Kaplan-Meier analyses of the probability of overall **(B, D)** or disease-free **(C, E)** survival in two groups of breast cancer patients based on the expression of the 16 relapse-associated miRs **(B, C)** or miR-148b **(D, E)**. Cluster 1 and 2 were obtained using the two major sample divisions achieved by the Unsupervised two-dimensional hierarchical clustering showed in **A (B, C)** or using miR-148b expression relative to the median value across all samples and a Receiver Operating Characteristic (ROC) curve to find the best separation among samples **(D, E)**. P values were calculated using Log Rank test.

Figure 1a

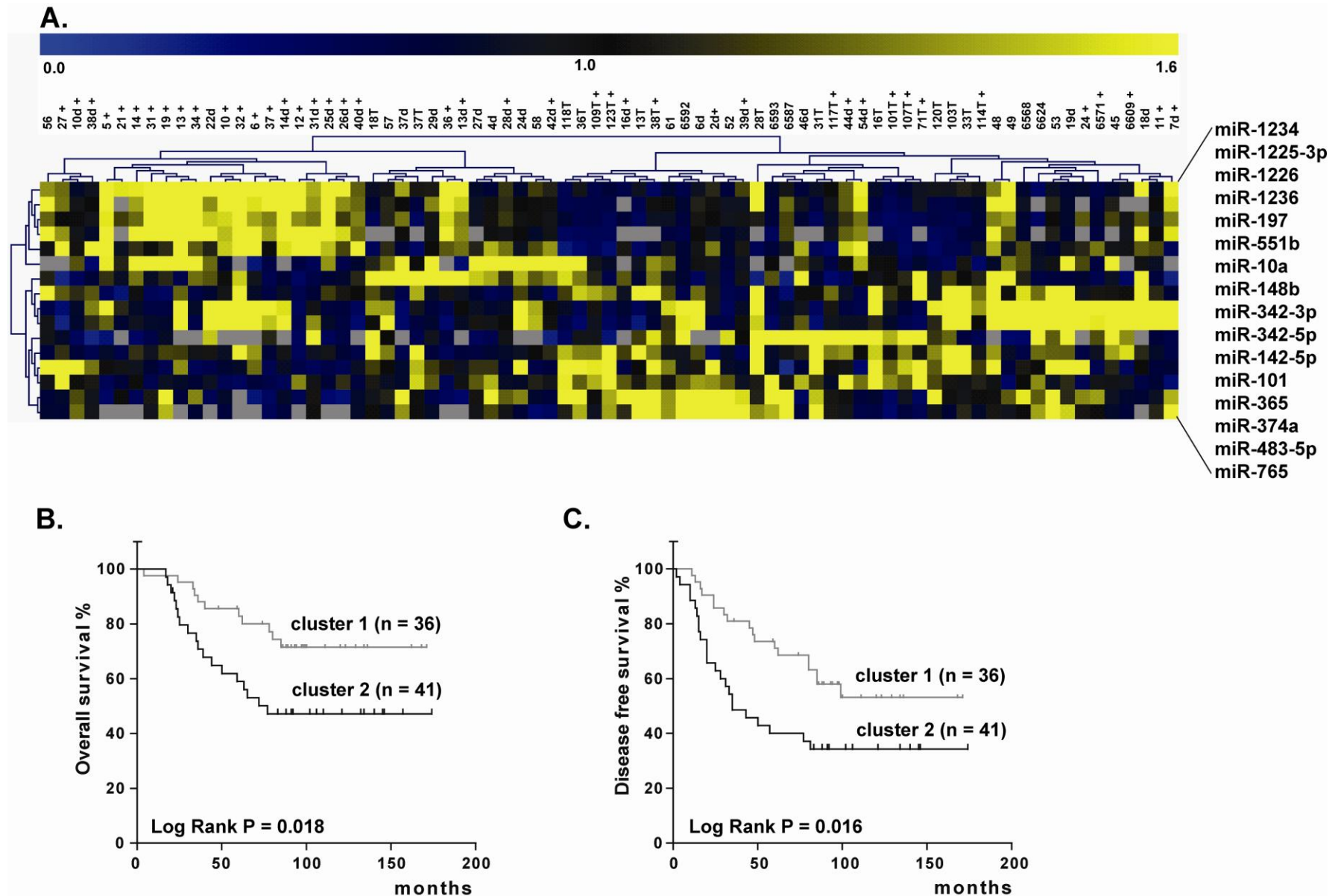
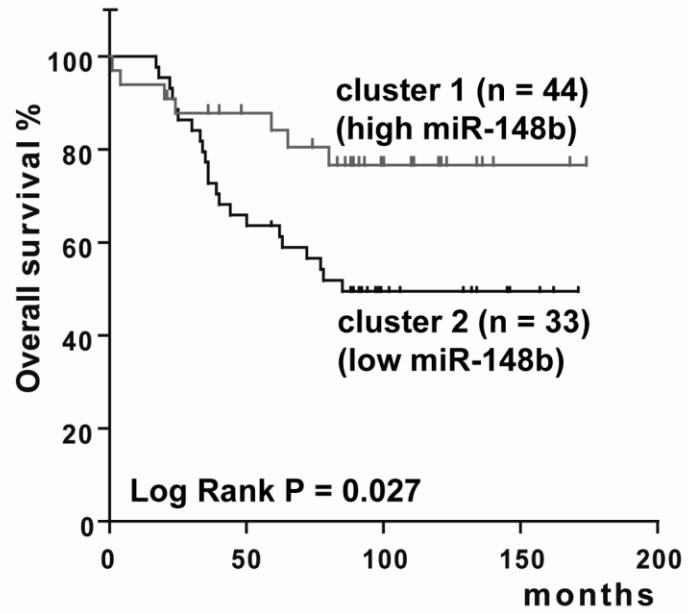
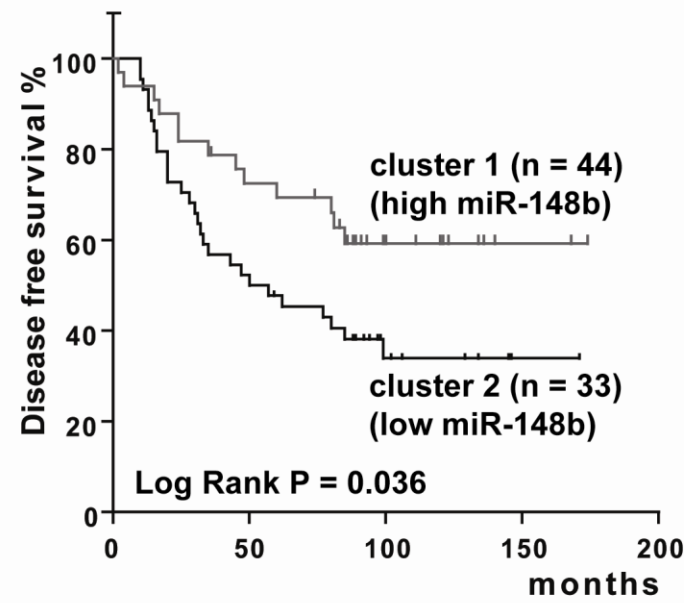


Figure 1b

**D.**



**E.**



**Figure 2 –Differentially expressed miRs comparing tumor samples from patients with (R+) or without disease relapse (R-) within 72 months.** Table (left) and graph (right) presenting the levels of expression of the 16 most modulated miRs in tumor samples from patients with (R+, n=41) versus without (R-, n=36) disease relapse. The Fold Change (FC) of R+/R- median values is shown in the Table. Instead, the averaged level of each miR in tumor samples versus mammoplastic reductions (controls) is shown as Log2 in the graph. False Discovery Rate (FDR): 16%.

Figure 2

Comparison between relapsing (R+, 41) and non-relapsing (R-, 36) samples [FDR=16%]

miR	R+/R- (FC)
miR-1238	2.15
miR-1228	1.87
miR-1225-3p	1.77
miR-1234	1.72
miR-197	1.62
miR-374a	-1.16
miR-101	-1.23
miR-365	-1.30
miR-765	-1.30
miR-551b	-1.33
miR-148b	-1.33
miR-483-5p	-1.40
miR-142-5p	-1.64
miR-342-3p	-1.71
miR-342-5p	-1.72
miR-10a	-1.96

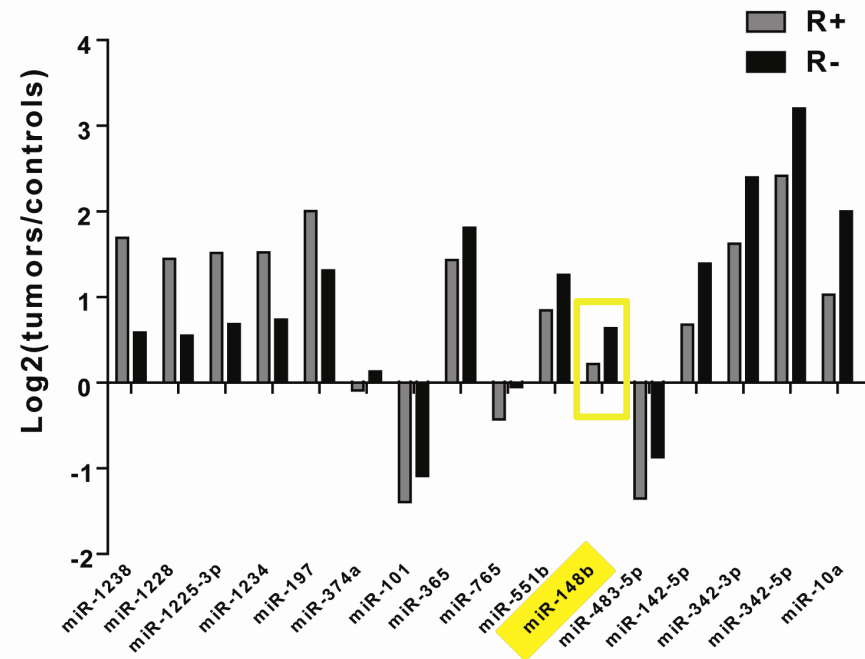


**Figure 3 – Differentially expressed miRs comparing estrogen receptor positive (ER+) and estrogen receptor negative (ER-) tumor samples.** Table (left) and graph (right) presenting the levels of expression of the 29 most modulated miRs in ER+ (n=53) versus ER- (n=24) tumor samples. The Fold Change (FC) of ER+/ER- median values is shown in the Table. Instead, the averaged level of each miR in tumor samples versus mammaplastic reductions (controls) is shown as Log2 in the graph. False Discovery Rate (FDR): 14%.

**Figure 3**

**Comparison between ER+ (53) and ER- (24) samples [FDR=14%]**

ID	ER+/ER- (FC)
miR-375	2.47
miR-342-3p	1.80
miR-142-5p	1.77
miR-181d	1.76
miR-21*	1.69
miR-202	1.54
miR-193a-3p	1.54
miR-29c	1.53
miR-148b	1.50
miR-29b	1.47
miR-141	1.46
miR-29c*	1.38
miR-199a-5p	1.34
miR-26a	1.31
miR-101	1.29
miR-155	-1.29
miR-146a	-1.31
miR-502-3p	-1.31
miR-197	-1.33
miR-532-5p	-1.39
miR-192	-1.39
miR-532-3p	-1.41
miR-146b-5p	-1.44
miR-223	-1.48
miR-150	-1.51
miR-125b-2*	-1.57
miR-505	-1.63
miR-486-5p	-1.68
miR-224	-1.94

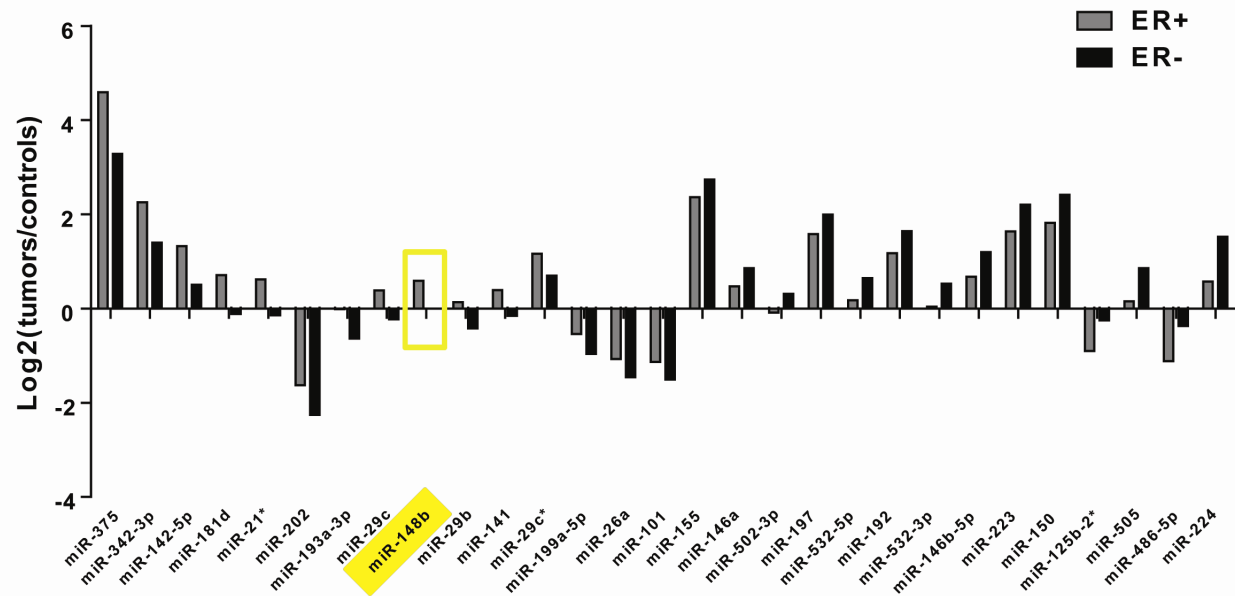


**Figure 4 – Differentially expressed miRs comparing progesterone receptor positive (PR+) and progesterone receptor negative (PR-) tumor samples.** Table (left) and graph (right) presenting the levels of expression of the 56 most modulated miRs in PR+ (n=42) versus PR- (n=35) tumor samples. The Fold Changes (FC) of PR+/PR- median values are shown in the Table. Instead, the averaged level of each miR in tumor samples versus mammoplastic reductions (controls) is shown as Log2 in the graph. False Discovery Rate (FDR): 9.30%.

Figure 4

ID	PR+/PR-
miR-30a	2.09
miR-30a*	2.07
miR-342-5p	2.03
miR-342-3p	1.75
miR-145	1.67
miR-145*	1.60
miR-29c*	1.55
miR-30c-2*	1.54
miR-95	1.52
miR-126*	1.52
miR-30c	1.51
miR-497	1.50
miR-154	1.47
miR-148b	1.46
miR-29c	1.45
miR-143	1.43
miR-101	1.40
miR-30e*	1.39
miR-181d	1.37
miR-376a	1.35
miR-199a-5p	1.34
miR-100	1.34
miR-139-5p	1.33
miR-195	1.32
miR-26a	1.30
miR-199b-5p	1.29
miR-361-5p	1.28
miR-149	1.26
miR-381	1.24
miR-874	-1.20
miR-25	-1.20
miR-766	-1.20
miR-1226*	-1.21
miR-150*	-1.23
miR-22	-1.24
miR-185	-1.24
miR-21	-1.25
miR-139-3p	-1.27
miR-33b*	-1.28
miR-146a	-1.28
miR-192	-1.30
miR-1225-5p	-1.34
miR-194	-1.35
miR-130b	-1.36
miR-198	-1.37
miR-574-5p	-1.38
miR-155	-1.51
miR-135a*	-1.62
miR-768-5p	-1.66
miR-801	-1.71
miR-663	-1.79
miR-18a	-1.83
miR-886-3p	-1.87
miR-210	-1.96
miR-7	-2.09
miR-224	-4.88

Comparison between PR+ (42) and PR- (35) samples [FDR=9.30%]

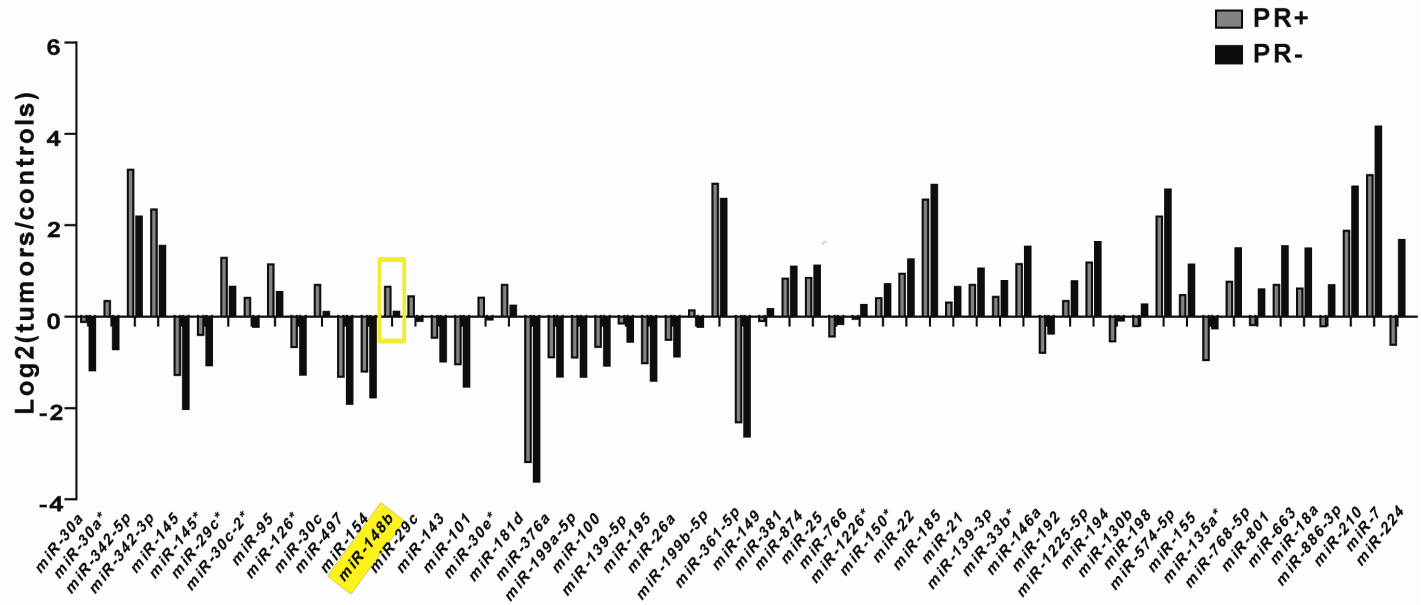
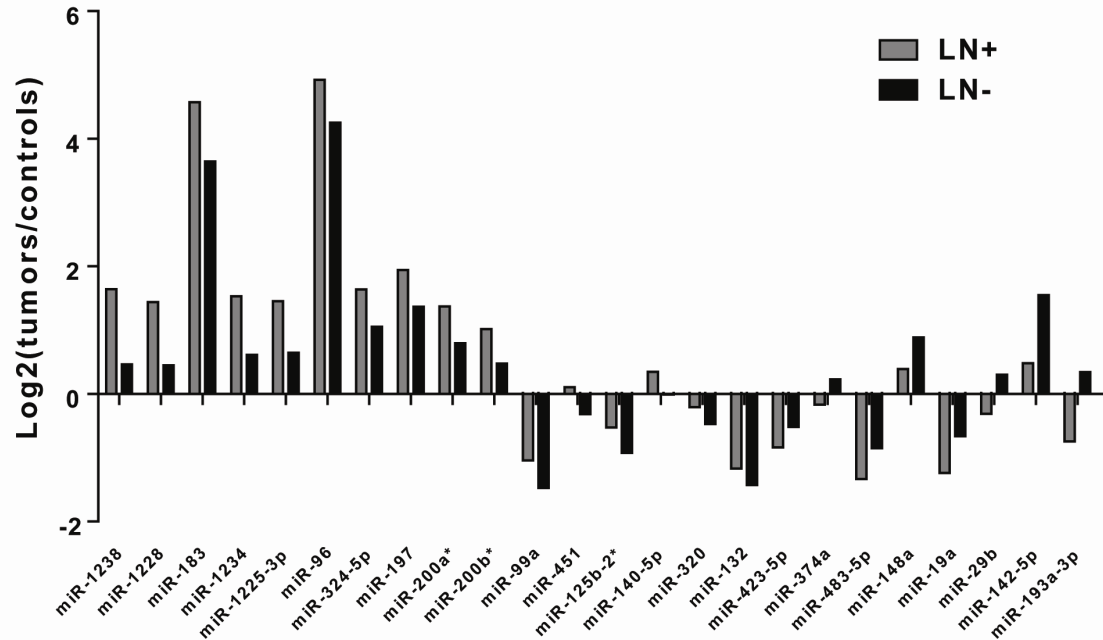


**Figure 5 – Differentially expressed miRs comparing lymph node positive (LN+) and lymph node negative (LN-) tumor samples.** Table (left) and graph (right) presenting the levels of expression of the 24 most modulated miRs in LN+ (n=44) versus LN- (n=33) tumor samples. The Fold Changes (FC) of LN+/LN- median values are shown in the Table. Instead, the averaged level of each miR in tumor samples versus mammoplastic reductions (controls) is shown as Log2 in the graph. False Discovery Rate (FDR): 7.6%.

Figure 5

Comparison between LN+ (44) and LN- (33) samples [FDR= 7.6%]

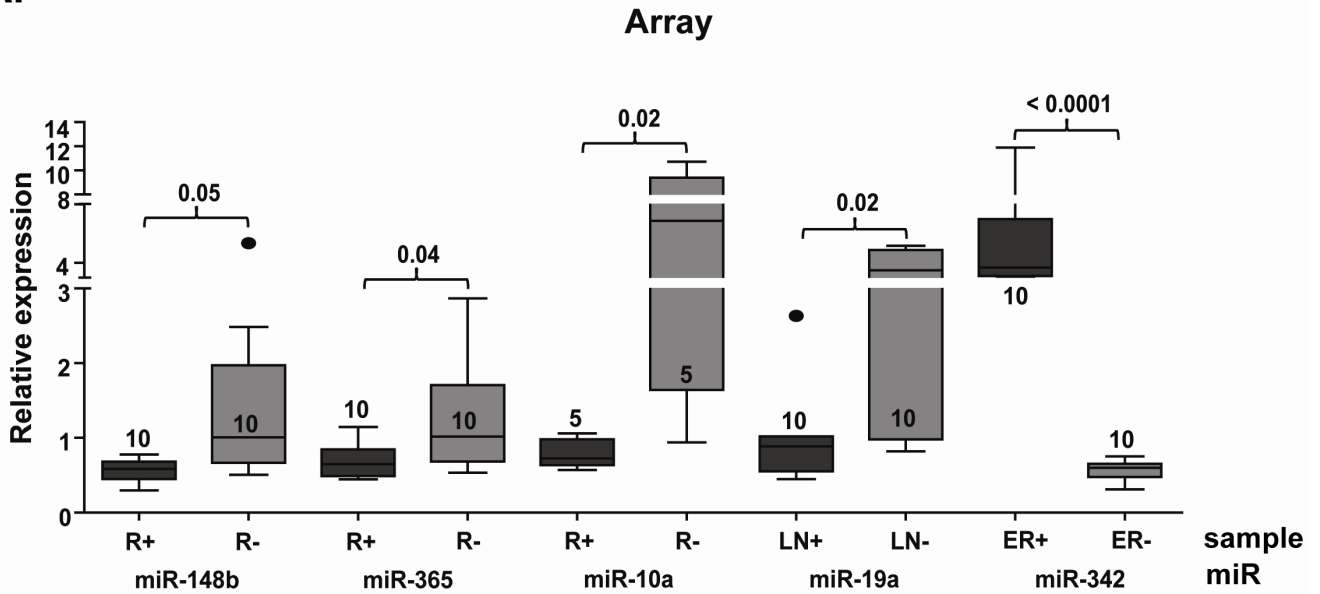
ID	LN+/LN-
miR-1238	2.26
miR-1228	1.99
miR-183	1.90
miR-1234	1.89
miR-1225-3p	1.75
miR-96	1.59
miR-324-5p	1.50
miR-197	1.49
miR-200a*	1.49
miR-200b*	1.45
miR-99a	1.35
miR-451	1.34
miR-125b-2*	1.32
miR-140-5p	1.28
miR-320	1.20
miR-132	1.20
miR-423-5p	-1.25
miR-374a	-1.31
miR-483-5p	-1.40
miR-148a	-1.40
miR-19a	-1.49
miR-29b	-1.53
miR-142-5p	-2.09
miR-193a-3p	-2.12



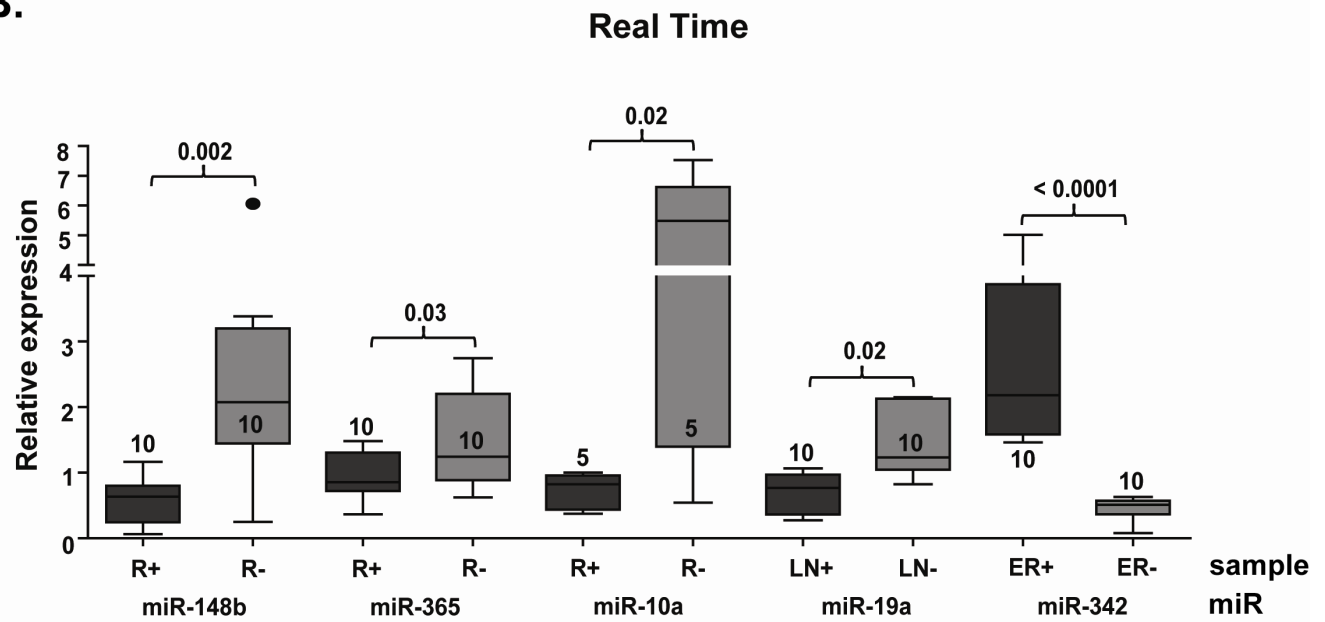
**Figure 6 – Validation of the miR microarray analysis results.** miR expression levels as obtained by microarray analysis **(A)** or qRT-PCR **(B)** shown by box-and-whisker plots. Normalized microarray or qRT-PCR data were expressed as fold changes relative to the median expression for each group of patients. For qRT-PCR, U44 RNA was used for normalization. The bottom and top of the box are the 1th and 3th quartile (the lower and upper quartile, respectively), the band in the middle of the box is the median and circles label outliers. The upper whisker shows the greatest value, the lower the least. The dots represent values more or less than 3/2 times of upper or lower quartile (Tukey method). R, relapse; LN, lymph node; ER, Estrogen Receptor; +, positive; -, negative. N=5 or 10 tumor samples per group. The two tailed Student's t test was used for comparisons and the p values are shown.

Figure 6

A.



B.

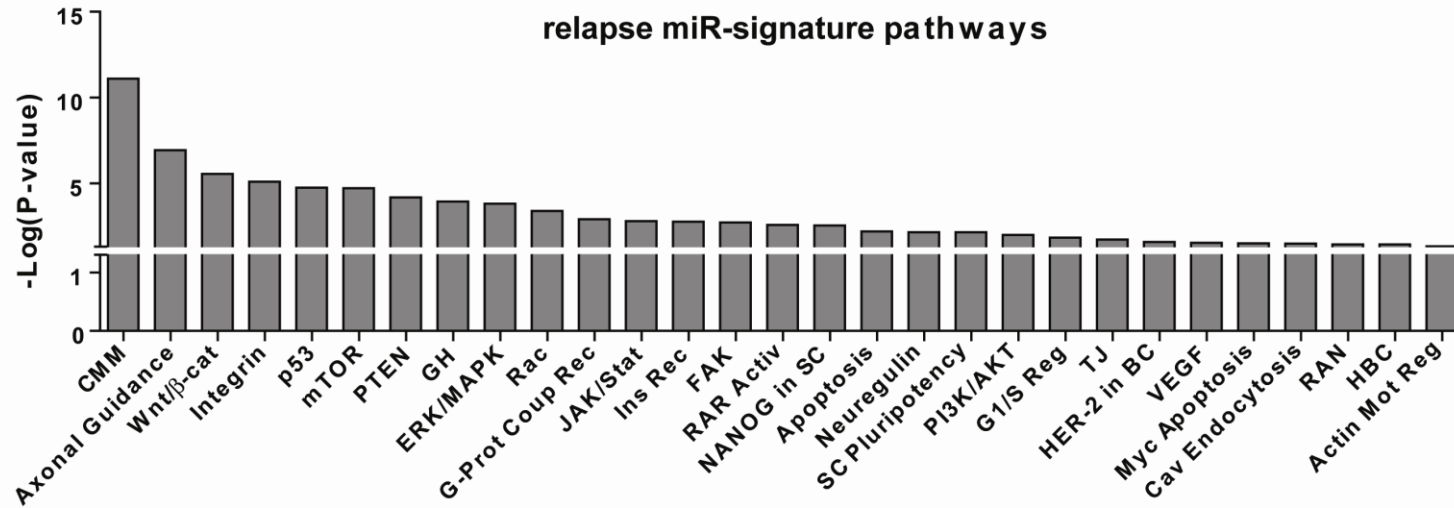


**Figure 7 – Pathway enrichment for relapse-associated or miR-148b putative targets.**

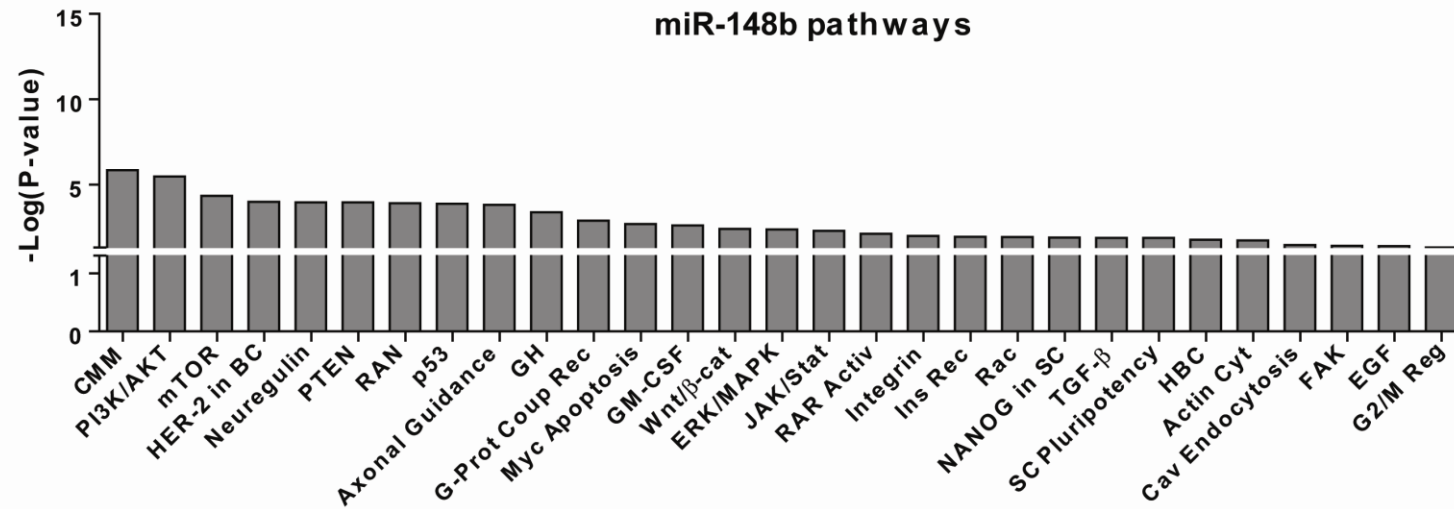
The miRecords System (<http://mirecords.biolead.org>) was used to predict miR targets; at least three different algorithms were considered. Pathway analysis was then performed for relapse-associated **(A)** or miR-148b **(B)** putative targets using the **Ingenuity Pathway Analysis Systems** (<http://www.ingenuity.com>) and enrichments were accepted when  $P < 0.05$  (Fisher test). Abbreviations: CMM, Cancer Molecular Mechanisms; Wnt/ $\beta$ -cat, Wnt/ $\beta$ -catenin; GH, Growth Hormone; G-Prot Coup Rec, G-Protein Coupled Receptor; Ins Rec, Insulin Receptor; RAR Activ, RAR Activation; NANOG in SC, Role of NANOG in stem cell; SC Pluripotency, Stem Cell Pluripotency; G1/S Reg, G1/S Checkpoint Regulation; T.J, Tight Junction; HER-2 in BC, HER-2 in Breast Cancer; Myc Apoptosis, Myc Mediated Apoptosis; Cav Endocytosis, Caveolar-mediated Endocytosis; HBC, Hereditary Breast Cancer Signaling; Actin Mot Reg, Actin-based Motility Regulation; Actin Cyt, Actin Cytoskeleton; G2/M Reg, G2/M Checkpoint Regulation.

Figure 7

A.



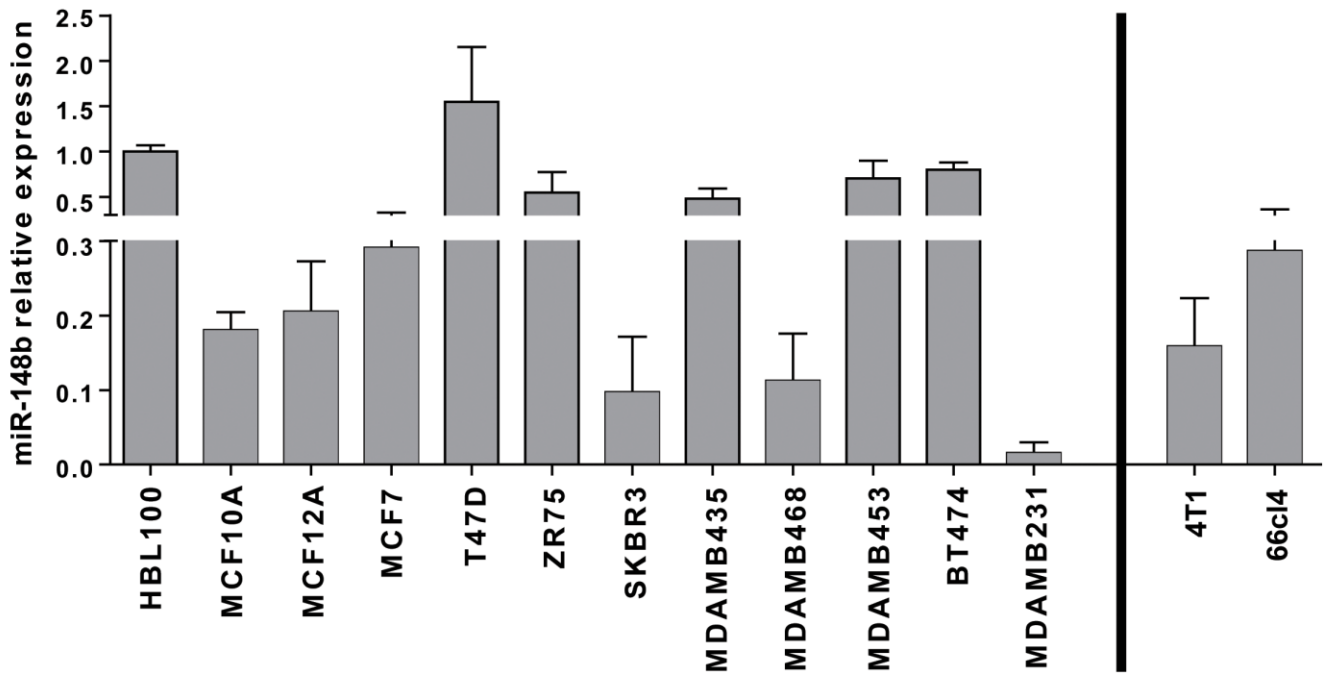
B.



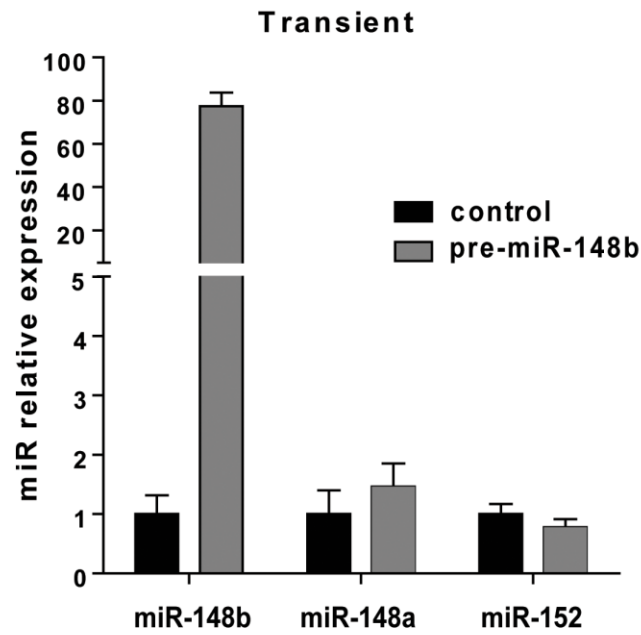
**Figure 8 – Analysis of miR-148b expression.** (A) miR-148b expression was evaluated for the indicated human or mouse tumor cell lines by qRT-PCR analysis. (B-C) qRT-PCRs were performed to evaluate miR-148b expression levels in MDA-MB-231 cells either transfected with miR-148b precursors or negative controls (pre-miR-148b or control) or stably transduced with pLemiR-empty or miR-148b overexpression vectors. Results were normalized on U44 RNA levels and presented as fold changes (mean $\pm$ STDEV) relative to miR-148b expression in HBL100 cells (A) or to controls (B, C). In B is also shown a representative analysis of the expression of other miR-148 family members (miR-148a and miR-152) in MDAMB231 miR-148b overexpressing cells (N=4).

Figure 8

A.

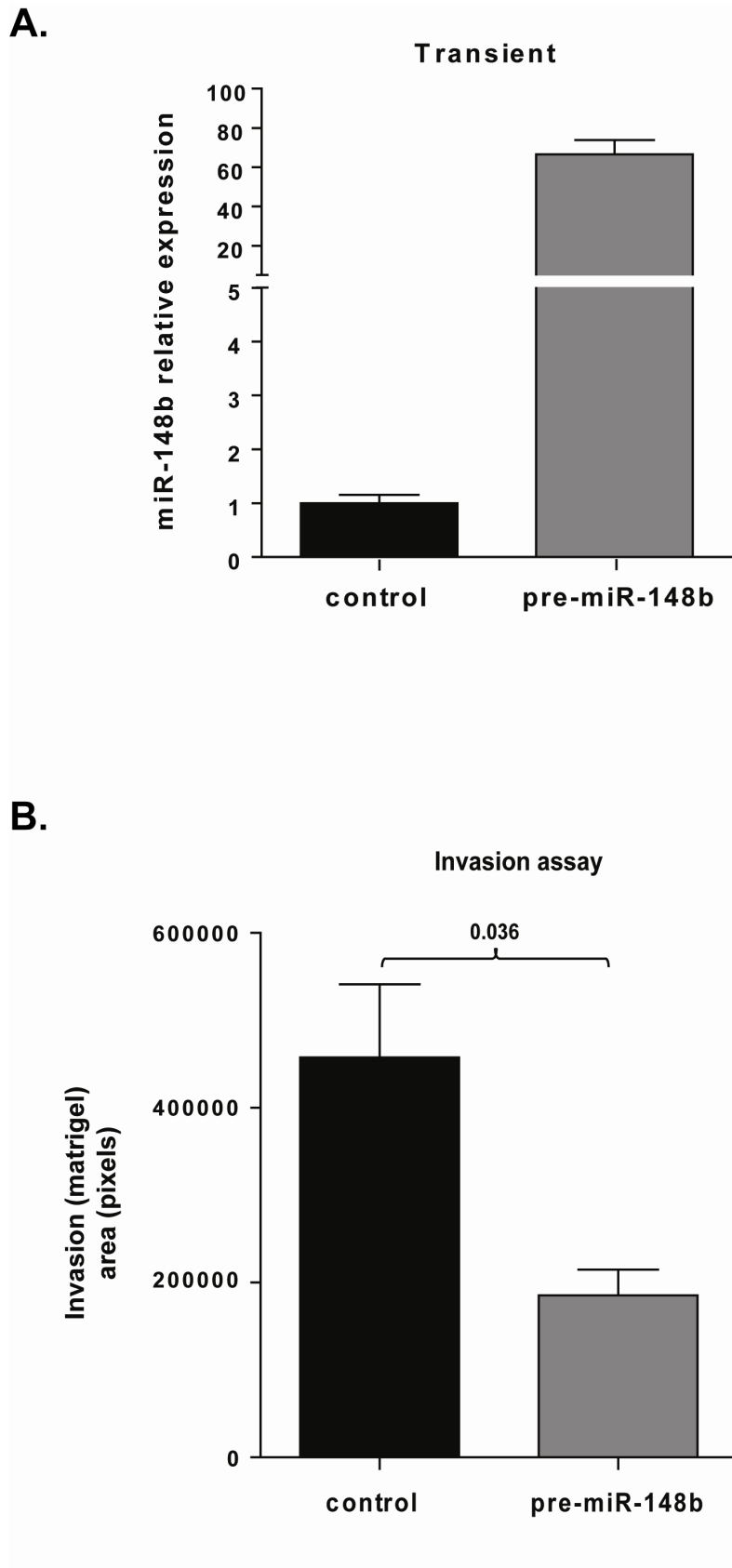


B.



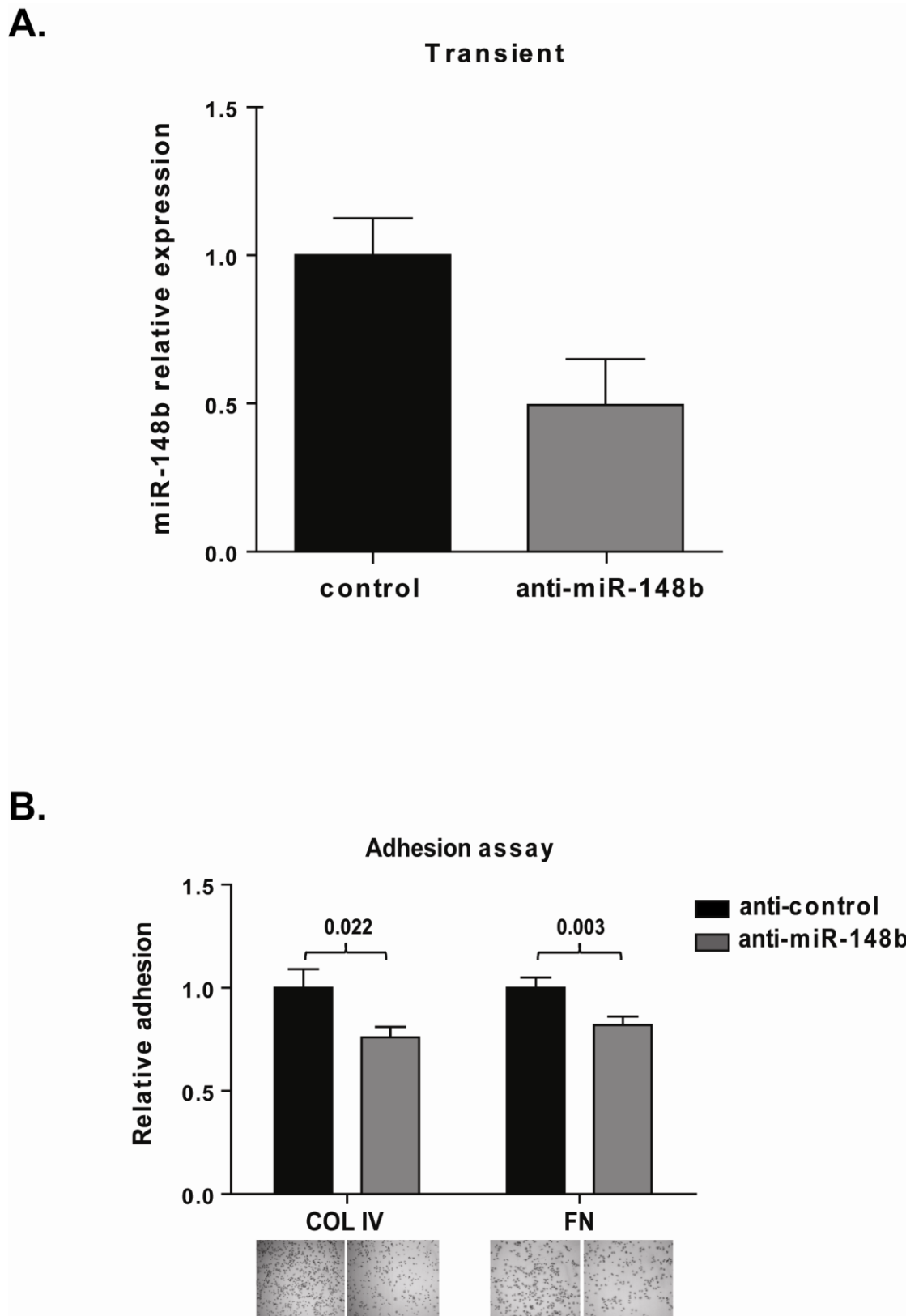
**Figure 9 - miR-148b affects 4T1 cell invasion.** 4T1 cells either transfected with miR-148b precursors or negative controls (pre-miR-148b or control) were used to evaluate miR-148b expression levels by qRT-PCRs, normalized on U44 RNA levels and presented as fold changes relative to controls **(A)** and perform transwell invasion through matrigel **(B)**. 3 independent experiments were performed in triplicate and representative results are shown as (mean±STDEV) of miR-148b expression or area covered by invading cells. The two tailed Student's t test was used for comparisons and the p value is shown.

Figure 9



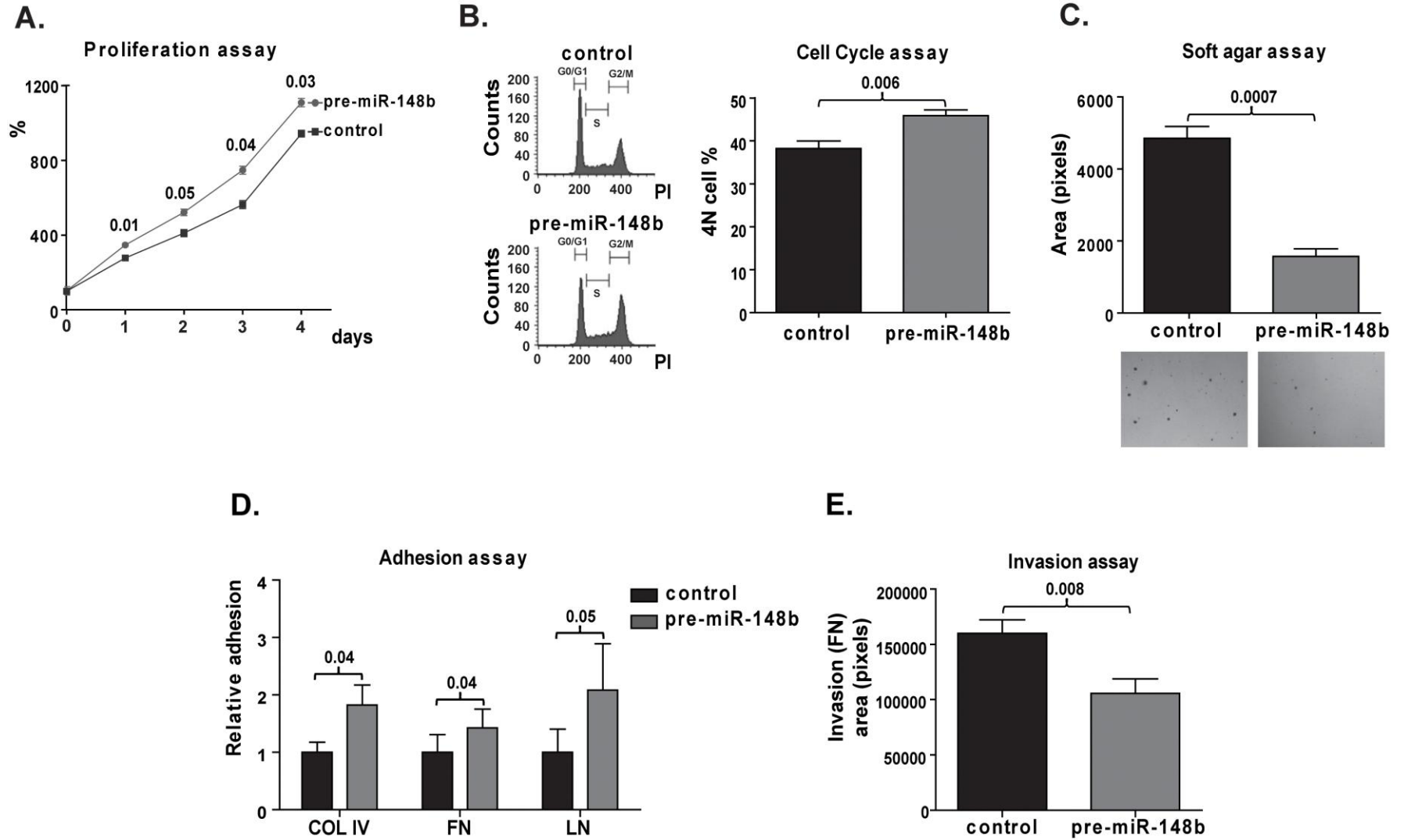
**Figure 10 - miR-148b affects MCF7 adhesion.** MCF7 cells either transfected with anti-miR-148b inhibitors or negative controls (anti-miR-148b or anti-control) were used to evaluate miR-148b expression levels by qRT-PCRs, normalized on U44 RNA levels and presented as fold changes relative to controls **(A)** and perform **(B)** adhesion on collagen IV (COLIV) or fibronectin (FN). 2 independent experiments were performed in triplicate and representative results are shown as (mean±STDEV) of miR-148b expression or area covered by adherent cells. The two tailed Student's t test was used for comparisons and the p values are shown.

Figure 10



**Figure 11 – miR-148b affects cell growth, adhesion and invasion.** Proliferation **(A)**, cell cycle **(B)**, anchorage-independent growth **(C)**, adhesion on collagen IV (COLIV), fibronectin (FN), laminin (LN) or FN-invasion **(D, E)** of MDA-MB-231 cells transfected with miR-148b precursors (pre-miR-148b) or its negative controls (control), or stably transduced with pLemiR-empty or miR-148b overexpression vectors. Results are shown as mean $\pm$ STDEV of the optical density of the increased proliferation (percentage, %) **(A)** or number of 4N (G2/M) cells (%) **(B)**, or area (pixels) covered by colonies **(C)**, or area covered by adherent **(D)** or FN-invasive **(E)** cells. Count of cells in G0/G1, S and G2/M were obtained by FACS analysis and are shown in **(B)**, referring to PI, Propidium Iodide, stained cells. 3-4 independent experiments were performed in triplicate and results are either shown as representative ones **(A, left panel in B, C)** or pooled together **(right panel in B, D, E)**. The two tailed Student's t test was used for comparisons and the p values are shown.

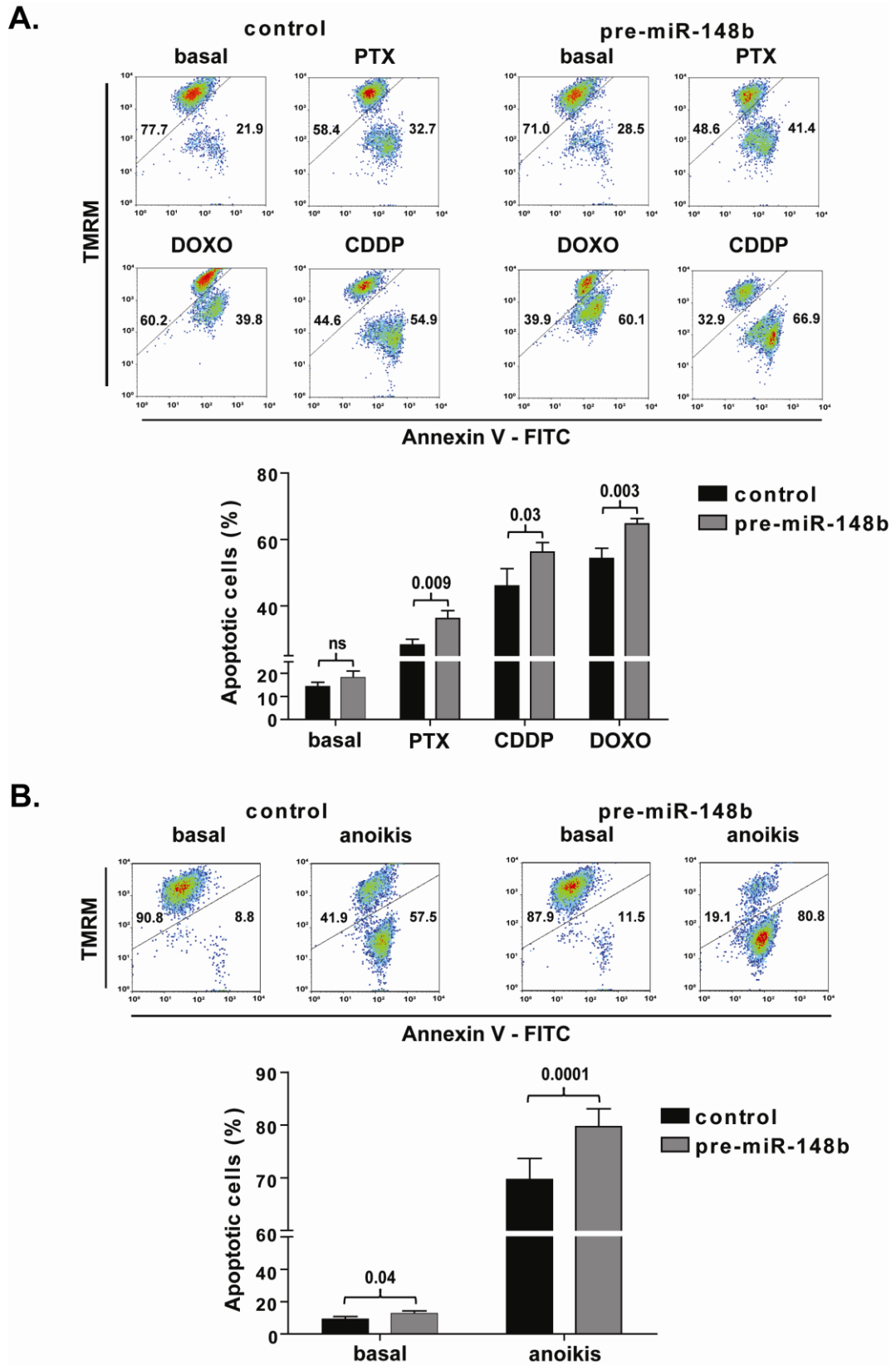
Figure 11



**Figure 12 – miR-148b affects chemotherapy-induced apoptosis and anoikis.**

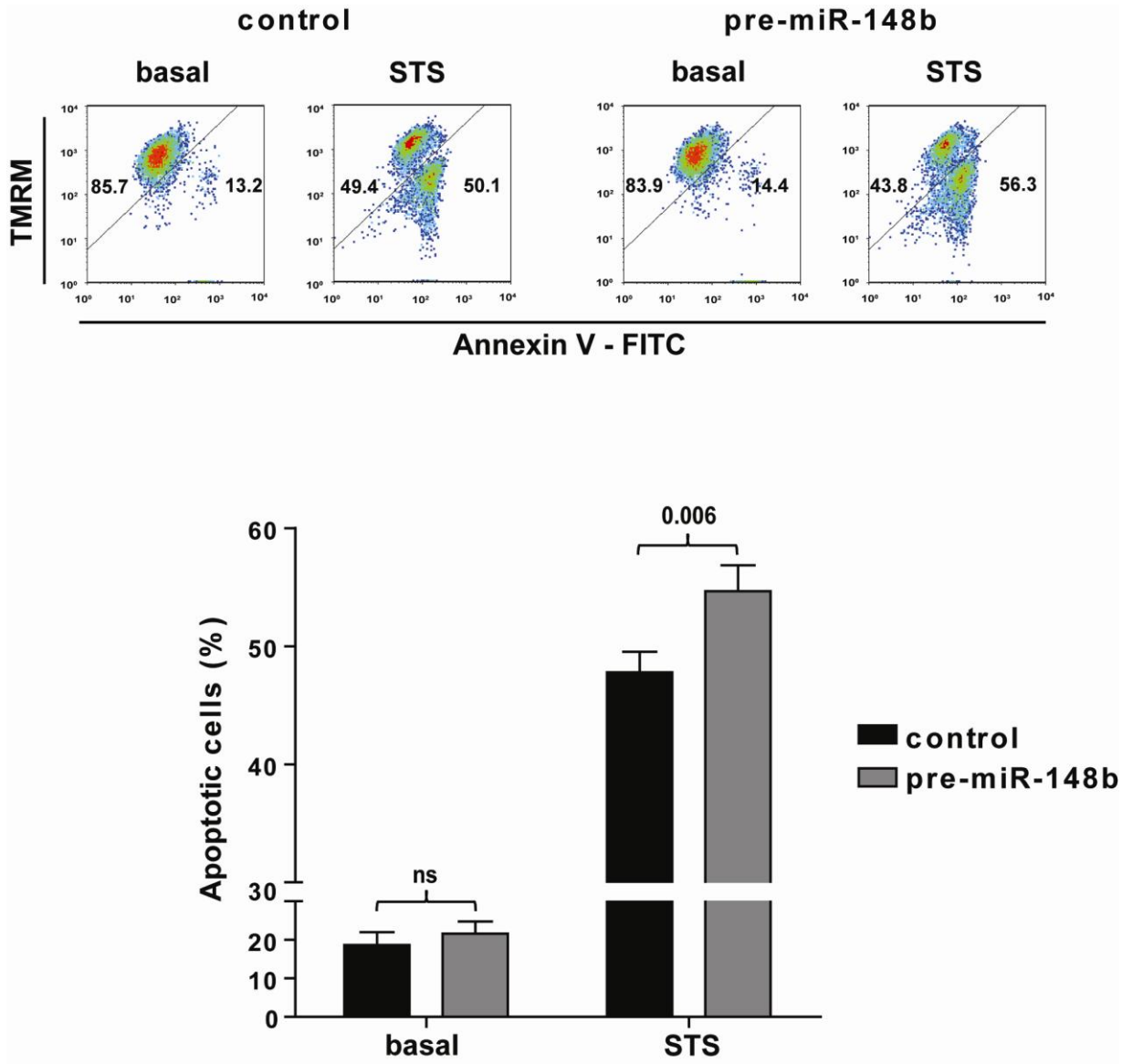
MDA-MB-231 cells transfected with miR-148b precursors (pre-miR-148b) or its negative controls (control) were grown in complete medium with or without Paclitaxel (PTX), Doxorubicine (DOXO) and Cis-Platin (CDDP) for 48h **(A)**. Alternatively the cells were kept in complete medium in presence or absence (anoikis) of attachment **(B)**. Cell death (apoptosis) percentage (%) was evaluated in **(A, B)** by TMRM and AnnexinV-FITC stainings and displayed in bidimensional plots. <sup>High</sup>TMRM-<sup>Low</sup>AnnexinV gate: healthy population; <sup>Low</sup>TMRM-<sup>High</sup>AnnexinV gate: apoptotic population. 3 independent experiments were performed in duplicate and a representative one is shown in plots; pooled quantitations show mean±SEM. The two tailed Student's t test was used for comparisons and the p values are shown.

Figure 12



**Figure 13 – miR-148b affects staurosporine induced apoptosis.** Apoptosis was analyzed in MDA-MB-231 cells either transfected with miR-148b precursors or negative controls (pre-miR-148b or control) following staurosporine (STS) treatment (25 ng/ml) for 48h by flow cytometry analysis. Cell death percentage (%) was evaluated by TMRM and AnnexinV-FITC stainings, displayed in bidimensional plots (representative experiment) and histograms. <sup>High</sup>TMRM-<sup>Low</sup>AnnexinV gate: healthy population; <sup>Low</sup>TMRM-<sup>High</sup>AnnexinV gate: apoptotic population. Three independent experiments were performed in duplicate and pooled quantitations are shown in the histograms as mean±SEM. The two tailed Student's t test was used for comparisons and the p values are shown.

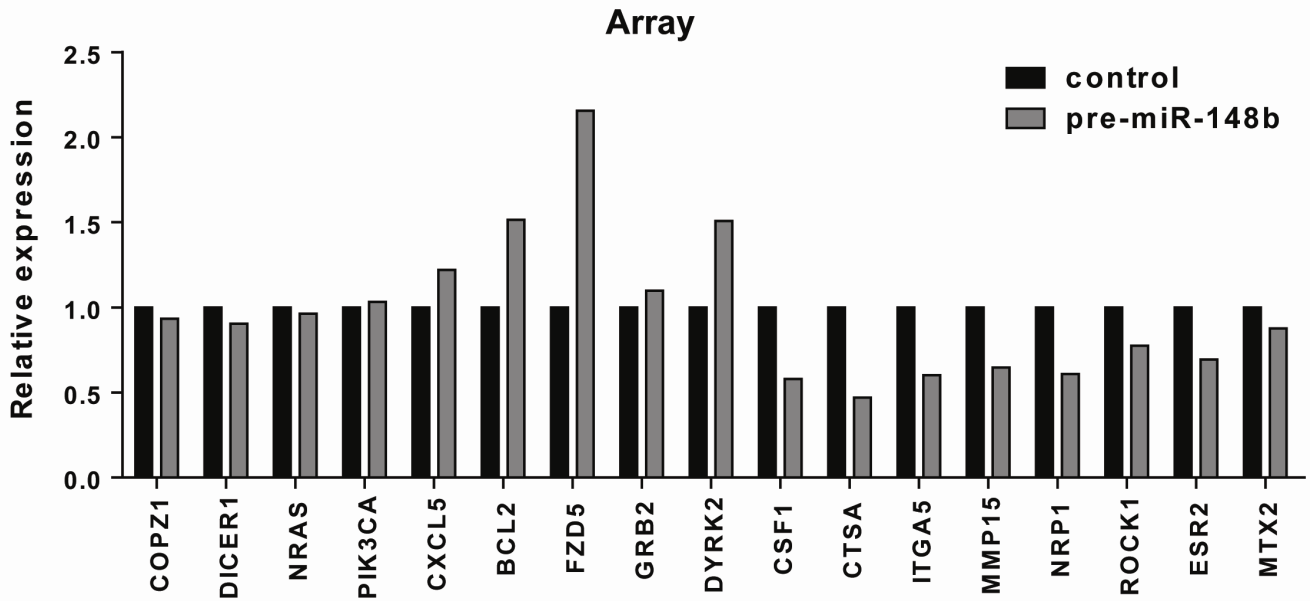
Figure 13



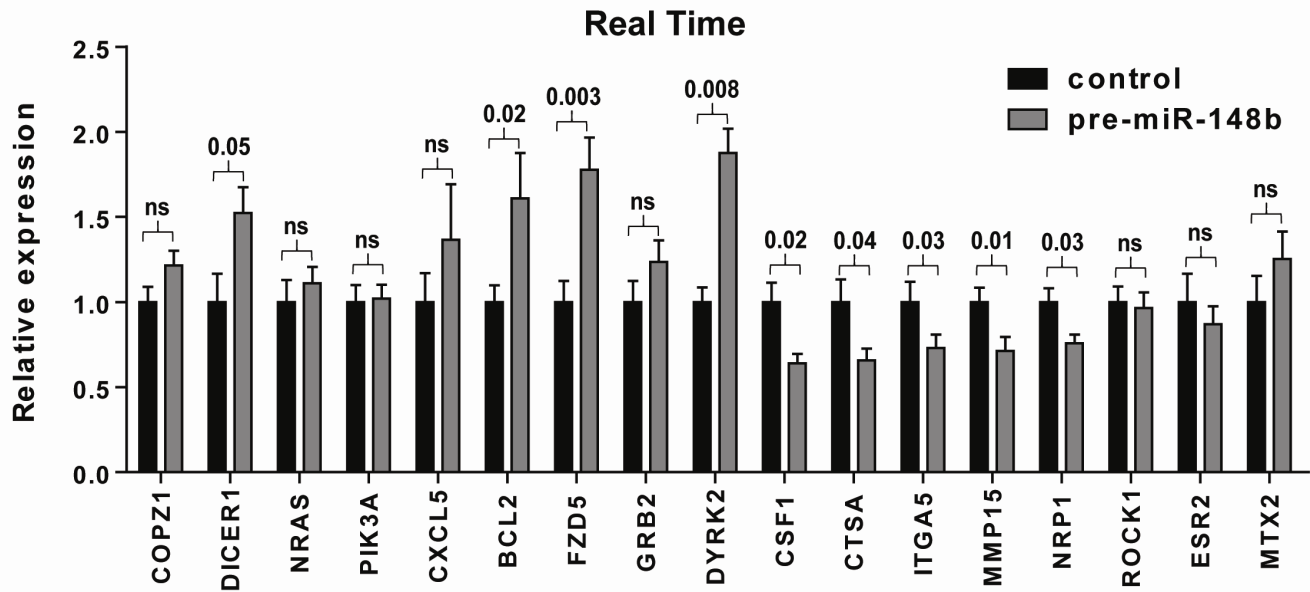
**Figure 14 – Validation of the protein-coding microarray analysis results.** MDA-MB-231 cells either transfected with miR-148b precursors or negative controls (pre-miR-148b or control) were used to perform a whole-genome microarray analysis and results of 17 randomly chosen protein-coding genes is displayed as gene expression fold changes referring to controls **(A)**. Validations of these 17 genes were performed by qRT-PCR analysis; results were normalized on 18S ribosomal RNA and calculated as gene expression fold changes (mean±STDEV) referring to the negative controls; N=3 **(B)**.

Figure 14

A.



B.



**Figure 15 – miR-148b modulates multiple genes.** MDA-MB-231 cells transfected with miR-148b precursors (pre-miR-148b) or its negative controls (control) were used 48 or 72 hours later to perform microarray analysis **(A)** or Western Blots **(B)** or Luciferase assays **(C, E)**.

**(A)** Unsupervised two-dimensional hierarchical clustering (Pearson correlation, average linkage) was performed for 33 putative miR-148b targets. Heatmap colors represent relative gene expression referring to the median transcription of genes across all samples, as indicated in the color key panel, median: black; row: protein-coding gene; column: cell sample. **(B)** Western Blot (WB) analysis was performed for four putative miR-148b targets, ITGA5, ROCK1, p110alpha and NRAS. Protein modulations were calculated relative to controls, normalized on the hsp90 loading control and expressed as percentages, 48 or 72 hours post-transfection. **(C)** Luciferase assays in cells transfected with reporter constructs containing the 3'UTR of the indicated genes or a synthetic sequence including 3 perfect miR-148b binding sites (sensor), cloned downstream of the Luciferase coding sequence. Results are shown as mean $\pm$ SEM of Firefly Luciferase activity relative to controls, normalized on Renilla Luciferase activity. **(D)** ITGA5 3' UTR. **(E)** Wild type and mutant miR-148b binding sites in ITGA5 3'UTR (ITGA5 $a$ mut and ITGA5 $b$ mut) paired with miR-148b seeds (left panel) and luciferase assays in cells transfected with wild type or mutant (a/b) ITGA5 3'UTR reporter constructs (right panel). 3 independent experiments were performed for **A** and **B**, with independent protein or RNA preparations. In **B** a representative one is shown. In **C** and **E** 3 independent experiments were performed in triplicate and results from one representative experiment are shown. The two tailed Student's t test was used for comparisons and the p values are shown.

Figure 15a

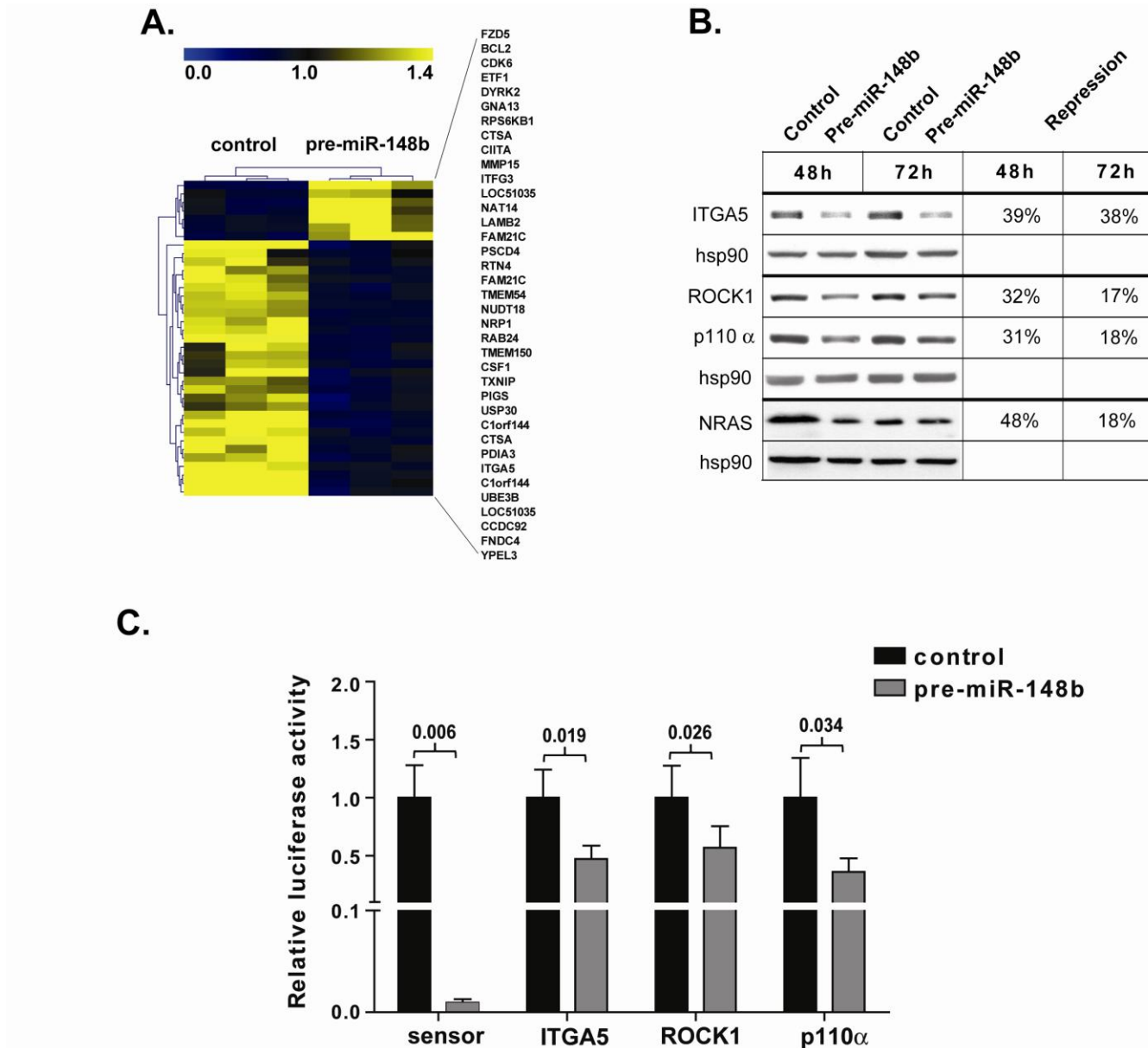
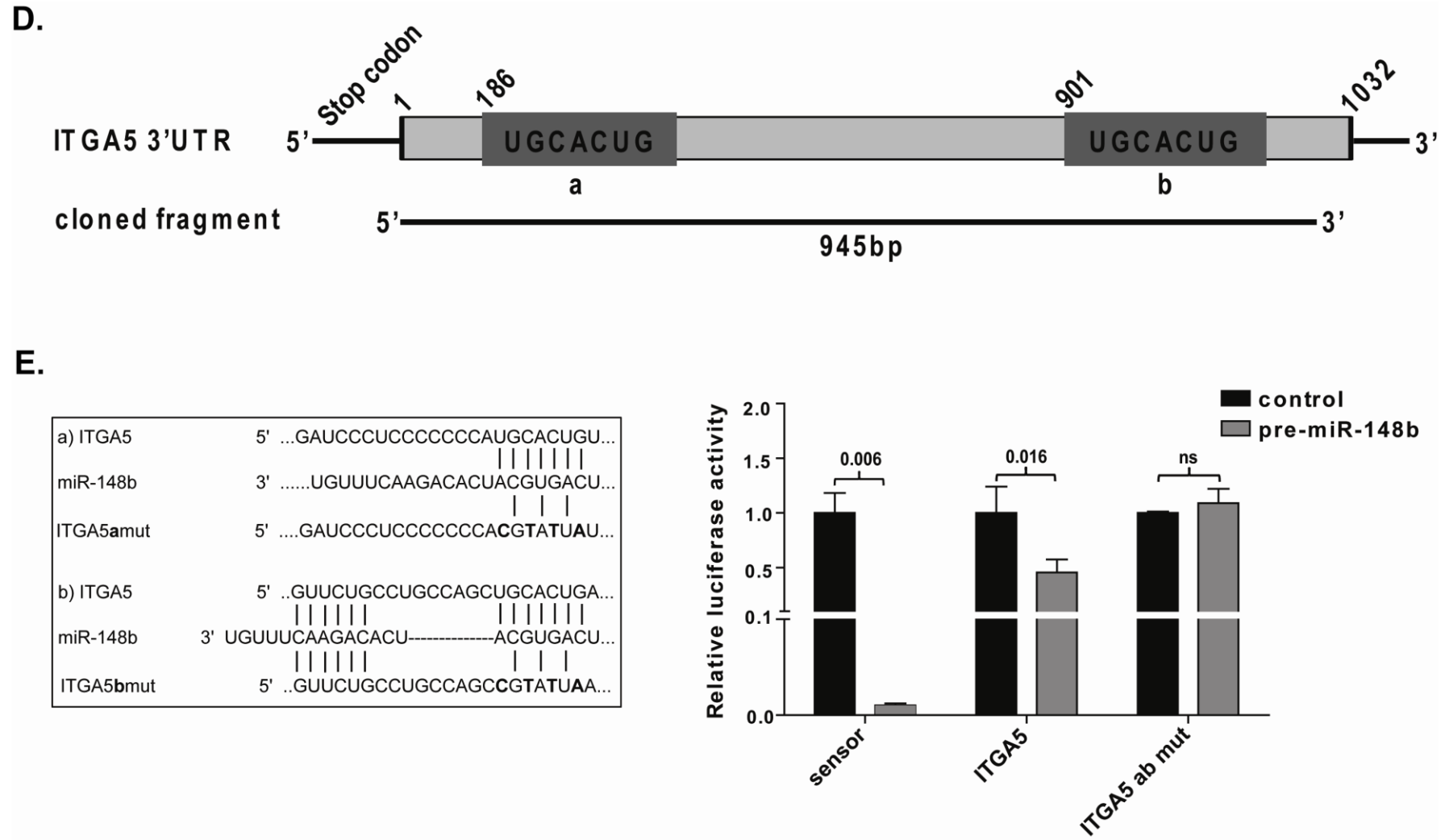


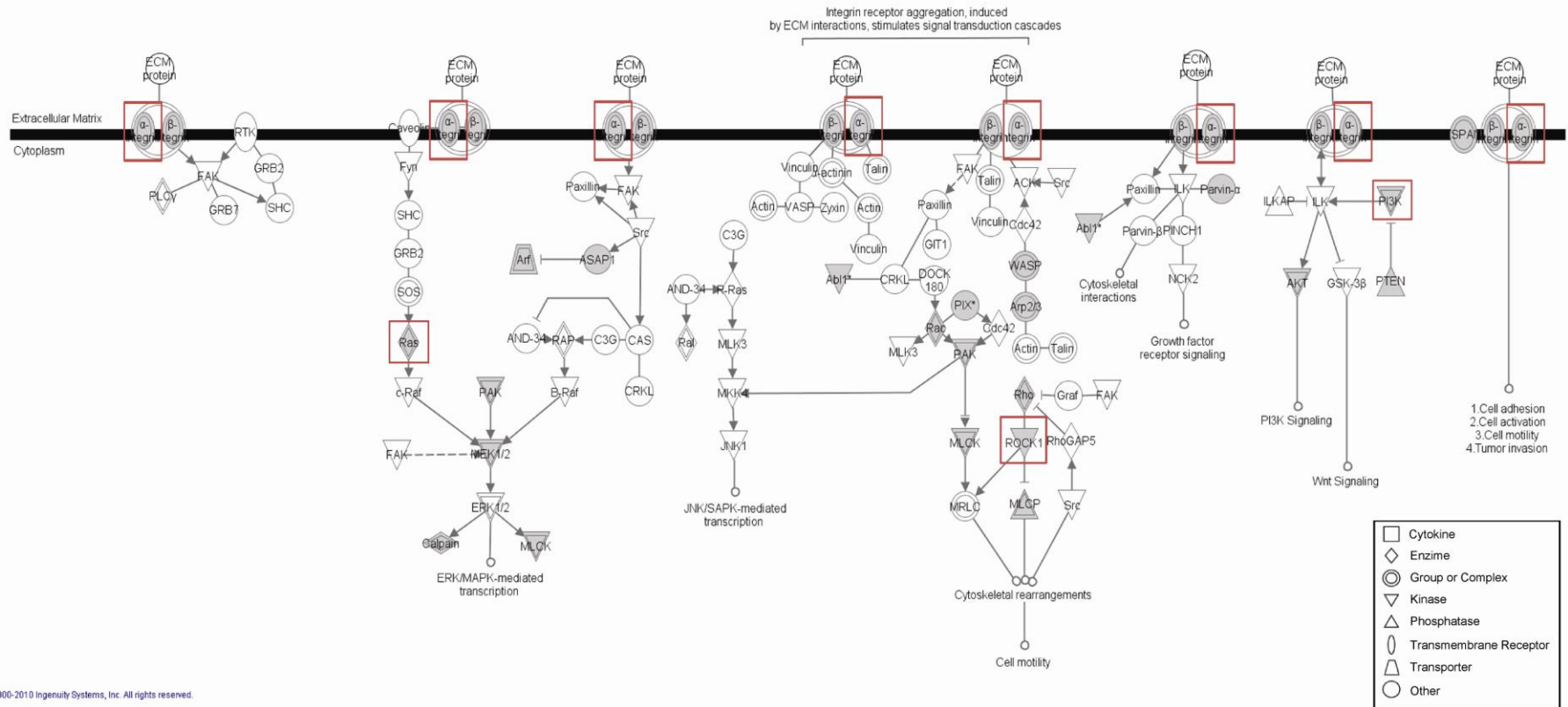
Figure 15b



**Figure 16 – Ingenuity Systems Analysis of miR-148b-modulated genes.** A total of 3642 miR-148b putative targets were obtained by miRecords algorithms and used to generate functional pathways employing the Ingenuity Pathway Analysis (IPA) Systems: the *Integrin signaling pathway* is shown here (enrichment p value 0.01). Gray shapes correspond to putative miR-148b targets. Red empty rectangles highlight miR-148b validated targets in this study following miR-148b overexpression (see figure 5).

Figure 16

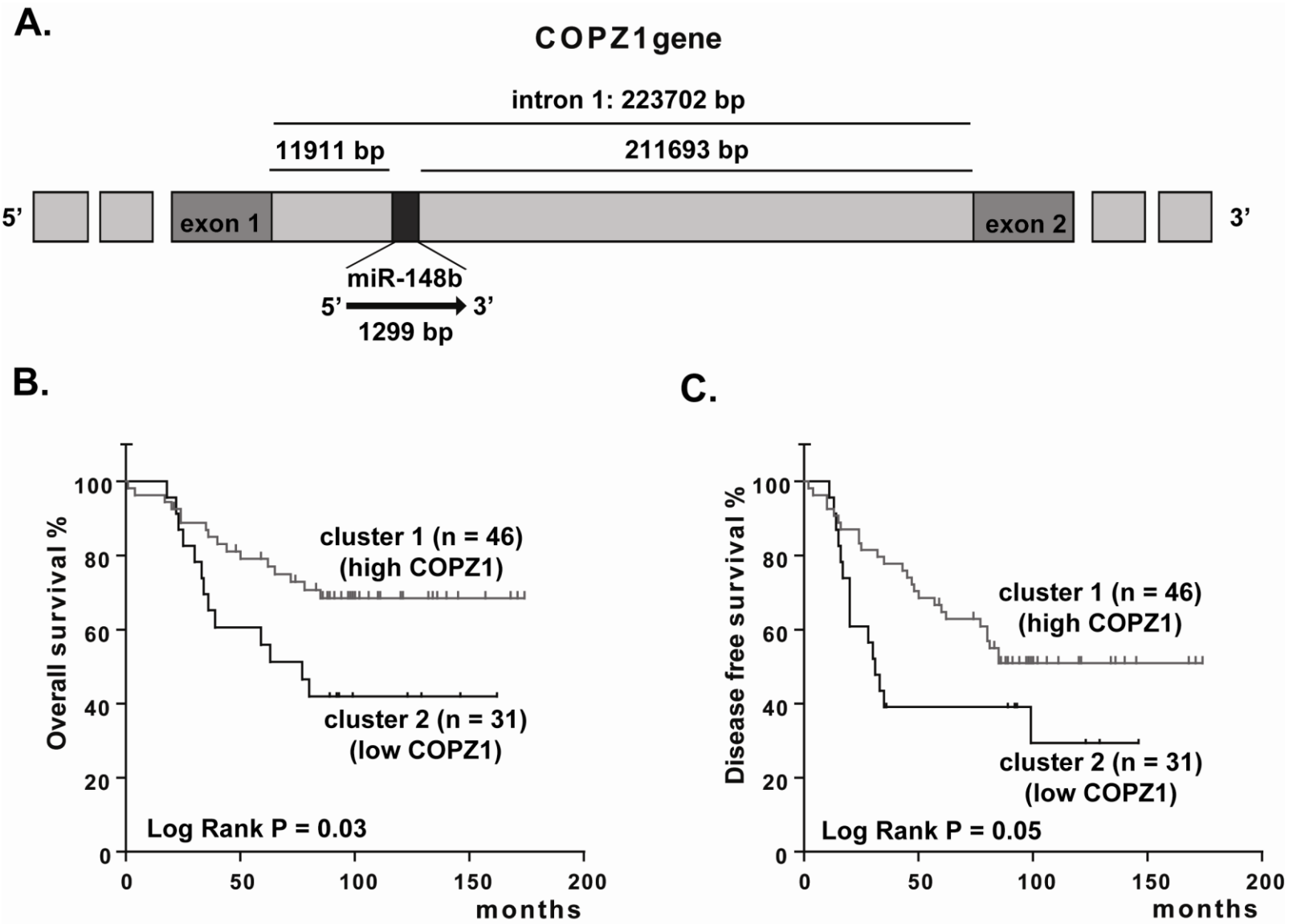
Integrin Signaling



© 2000-2010 Ingenuity Systems, Inc. All rights reserved.

**Figure 17 – COPZ1, the miR-148b-host gene, associates with overall or disease free survival (A)** miR-148b is located in the COPZ1 intron 1 (Chromosome 12: 54,718,911-54,745,633 forward strand); sequence information obtained from Ensamble and AceView databases. **(B)** Kaplan-Meier analyses of the probability of overall **(B)** or disease-free **(C)** survival in two groups of breast cancer patients according to COPZ1 expression as obtained by qRT-PCR. Results were normalized on the 18S ribosomal RNA and calculated as fold changes relative to the median expression of COPZ1, high (n=46) and low (n=31) expression. Receiver Operating Characteristic (ROC) curves were used to find the best separation among samples. P=0.03 **(B)**; P=0.05 **(C)**.

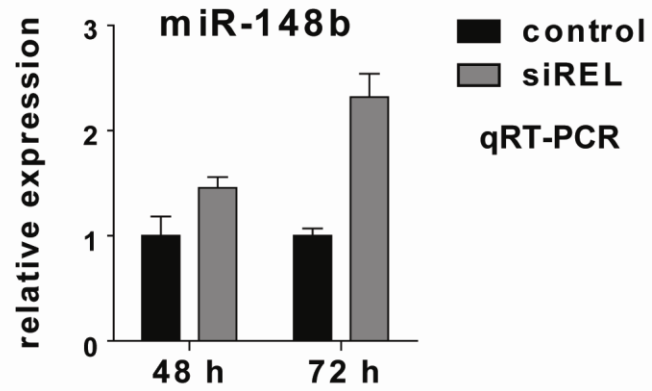
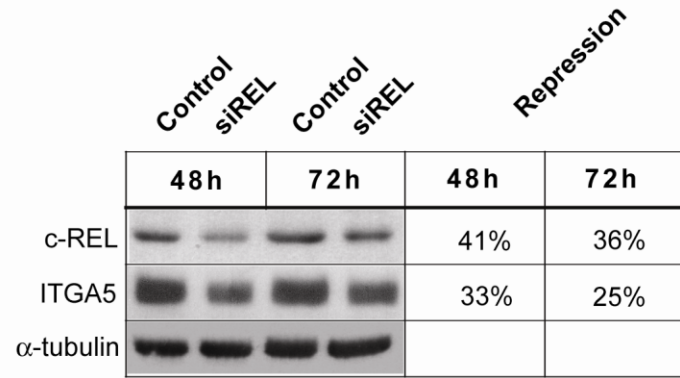
Figure 17



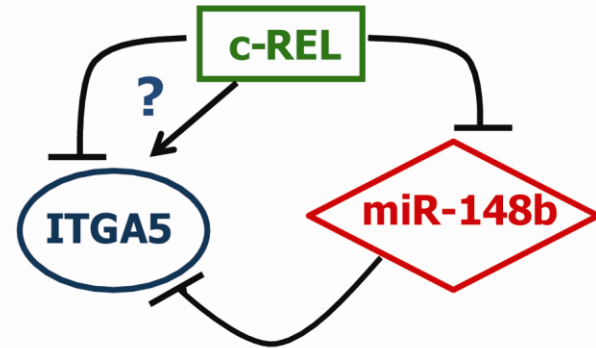
**Figure 18 – miR-148b and ITGA5 are part of a mixed Feed-Forward Loop (FFL) with the c-REL transcription factor.** (A) MDA-MB-231 cells transfected with REL-targeting or negative control siRNAs (siREL or control) were used 48 or 72 hours later to perform Western Blot (WB) analysis for c-REL and ITGA5 (upper panel). Protein modulations were calculated relative to controls, normalized on the  $\alpha$ -tubulin loading control and expressed as percentages (%) of repression. The level of miR-148b was evaluated by qRT-PCR (lower panel) and modulations were calculated relative to siRNA-negative controls, normalized on the U44 RNA level. 2 independent experiments were performed in duplicate and a representative one is shown; miR-148b quantitations are shown as mean $\pm$ STDEV. (B) Representation of the miR-148b-ITGA5-C-REL FFL; symbols:  $\perp$ , repression;  $\rightarrow$ , activation; ?, not known yet.

Figure 18

A.



B.



# TABLES

**Table 1. Clinical characteristics of the patients**

N, number; %, percentage; LN, lymph node; ER, Estrogen Receptor; PR, Progesteron Receptor; \*, ER and PR are defined positive when tumors contain more than 10 fmol/mg protein or minus than 10% positive tumor cells.

**Table 1:** Clinical characteristic of the patients.

Characteristics		N	%
<b>Tumor samples</b>			
<b>Number of patients</b>		77	
<b>Age (years)</b>	<b>median</b>	54	
	<b>range</b>	25- 82	
<b>Tumor Stage</b>	1	20	26.0
	2	51	66.2
	3	3	3.9
	4	3	3.9
<b>Tumor Grade</b>	1	4	5.2
	2	35	45.4
	3	33	42.8
	Unknown	5	6.5
<b>LN</b>	<b>Positive</b>	44	57.1
	<b>Negative</b>	33	42.9
<b>ER*</b>	<b>Positive</b>	53	68.8
	<b>Negative</b>	24	31.2
<b>PR*</b>	<b>Positive</b>	42	54.5
	<b>Negative</b>	35	45.4
<b>Relapse (72 months)</b>	<b>yes</b>	41	53.2
	<b>no</b>	36	46.7
<b>Normal samples</b>			
<b>Number of patients</b>		13	
<b>Age (years)</b>	<b>median</b>		
	<b>range</b>		

N, number; %, percentage, LN: Lymph node status, ER: Estrogen receptor status, PR: Progesterone receptor status.

\* ER and PR are defined positive when tumors contain more than 10 fmol/mg protein or minus than 10% positive tumor cells.

**Table 2. Classification power of Relapse-associated miRs compared with lymph node invasion.** The 16 differentially expressed miRs considering Relapse + or – patients (16 miR-signature) was used to classify samples within our group or within Blenkiron et al. set of patients (28). Comparison with lymph node (LN) classification is shown.

**Table 2.** Classification power of Relapse-associated miRs compared with lymph node invasion.

Dataset	miRs		LN	
	Good*	Poor**	Good*	Poor**
Our dataset	88% ± 15	76% ± 18	72% ± 21	85% ± 15
Blenkiron et al.(1)	76% ± 17	40% ± 25	72% ± 18	60% ± 25

Note: The 16 differentially expressed miRs considering Relapse + or – patients (16 miR-signature) was used to classify samples within our group or within Blenkiron et al. set of patients (8). Percentages of good prognosis samples correctly classified with 95% confidence interval (CI) (\*), or poor (\*\*), are shown in comparison with lymph node (LN) percentages classification.

**Table 3. Percentage (%) of target genes potentially modulated by each miR.**

Target prediction algorithm: miRecords System, 3 algorithm cut. %, percentage. R+, positive or R-, negative relapse.

**Table 3:** Percentage (%) of target genes potentially modulated by each miR.

	miR	Total target %	
Down in R+	miR-765	38.1	
	miR-148b	25.1	
	miR-342-5p	21.8	
	miR-342-3p	20.0	
	miR-101	17.6	
	miR-142-5p	16.8	
	miR-483-5p	15.6	
	miR-10a	13.6	
	miR-365	10.1	
	miR-374a	10.0	
	miR-551b	4.8	
	Up in R+	miR-197	23.6
		miR-1225-3p	15.8
miR-1228		15.4	
miR-1238		9.8	
miR-1234		9.5	

NOTE: Considering the 16 relapse-associated miRs, a target prediction analysis was performed using the miRecords System (<http://mirecords.umn.edu>) (3 algorithm cut) and a combined list of putative targets was obtained. In this table the percentage (%) of genes targeted by each relapse-associated miR is shown. R+, positive relapse.

**Table 4: miR-148b modulated protein-coding genes.** MDA-MB-231 cells either transfected with miR-148b precursors or negative controls (pre-miR-148b or control) were used to perform a microarray analysis (Whole Human Genome Oligo Microarray”, Agilent). Up- and down-modulated protein-coding genes considering: minimum fold change (FC)=1.5; false discovery rate (FDR)=16%.

**Table 4:** miR-148b modulated protein-coding genes

Down			Up		
ProbeName	GeneName	pre-miR-148b vs control*	ProbeName	GeneName	pre-miR-148b vs control*
A 24 P255114	ENST00000299512	-2.18	A 32 P68148	ZNF738	1.50
A 23 P311912	AHNAK2	-2.12	A 32 P81334	LARP4	1.50
A 24 P74371	CTSA	-2.12	A 23 P204048	DYRK2	1.51
A 24 P74374	CTSA	-2.10	A 24 P551028	LOC339745	1.51
A 23 P103496	GBP4	-2.02	A 23 P352266	BCL2	1.51
A 24 P259276	ZDHHC24	-1.96	A 23 P432034	CCDC117	1.52
A 32 P97798	AU184995	-1.94	A 24 P247044	ENST00000355095	1.54
A 23 P62768	TMEM54	-1.92	A 24 P752362	A 24 P752362	1.54
A 24 P845223	M27126	-1.90	A 24 P22657	AK096415	1.55
A 23 P99883	PDIA3	-1.90	A 23 P400580	KIAA1450	1.55
A 24 P273253	AHNAK2	-1.86	A 24 P769672	KRTHB5	1.56
A 24 P291401	TMEM150	-1.85	A 23 P404606	LOC153222	1.58
A 23 P31006	HLA-DRB5	-1.85	A 24 P295452	ROD1	1.58
A 24 P258277	LOC51035	-1.85	A 24 P5935	Kua-UEV	1.61
A 23 P97700	TXNIP	-1.84	A 23 P167269	FLJ11184	1.62
A 23 P346093	TMC8	-1.81	A 23 P110184	SC4MOL	1.62
A 23 P144622	GNPDA1	-1.81	A 32 P95914	C6orf167	1.62
A 23 P21207	UBE1L	-1.80	A 24 P263776	MST101	1.63
A 23 P66715	PIGS	-1.80	A 32 P194779	ZBTB34	1.63
A 23 P76829	HOMEZ	-1.79	A 23 P144916	GFPT2	1.63
A 24 P57528	SLC39A11	-1.77	A 23 P35376	NHLRC2	1.64
A 23 P49467	C1orf144	-1.77	A 24 P80776	AK129879	1.64
A 23 P15108	YPEL3	-1.75	A 32 P234827	ARMC1	1.65
A 23 P257164	AMT	-1.72	A 24 P943888	GRWD1	1.65
A 23 P407012	CSF1	-1.72	A 23 P133582	ETF1	1.66
A 23 P66117	ITFG3	-1.72	A 23 P145397	CCNC	1.68
A 24 P71700	ZBTB47	-1.71	A 23 P86623	ENTPD7	1.71
A 24 P402222	HLA-DRB3	-1.71	A 24 P372217	ERLIN2	1.72
A 23 P98900	CCDC92	-1.69	A 24 P402836	ZNF141	1.73
A 23 P42306	HLA-DMA	-1.68	A 32 P137604	BC018597	1.74
A 23 P429046	RP11-56A21.1	-1.68	A 23 P104138	MGC15634	1.74
A 24 P172481	TRIM22	-1.67	A 24 P941441	GNA13	1.75
A 23 P36562	ITGA5	-1.66	A 23 P121064	PTX3	1.76
A 32 P217773	SYTL1	-1.66	A 24 P166663	CDK6	1.76
A 32 P422453	FAM21C	-1.66	A 23 P501996	Kua-UEV	1.81
A 23 P150249	CCDC85B	-1.66	A 24 P112447	ENTPD7	1.84
A 23 P85800	CD52	-1.66	A 23 P94095	ANKRD46	1.84
A 32 P122373	MSTP9	-1.64	A 24 P521409	RPS6KB1	1.84
A 24 P928052	NRP1	-1.64	A 24 P118862	ZNF678	1.84
A 23 P50389	NAT14	-1.64	A 24 P358868	LOC388523	1.91
A 24 P50245	HLA-DMA	-1.62	A 32 P207789	BQ017638	1.95
A 23 P98605	LOC51035	-1.62	A 32 P190737	KIAA1450	2.01
A 23 P99186	UBE3B	-1.62	A 24 P778836	RSL1D1	2.02
A 23 P16834	FNDC4	-1.61	A 24 P162319	SCML1	2.06
A 23 P67151	OLFM2	-1.61	A 23 P165239	ZNF208	2.12
A 23 P155057	PSCD4	-1.60	A 32 P158723	AK123861	2.15
A 24 P513764	A 24 P513764	-1.60	A 23 P108437	FZD5	2.16
A 23 P254353	NOXA1	-1.60	A 32 P43826	AL832540	2.18
A 23 P411379	C6orf1	-1.59	A 23 P60210	RLN1	2.37
A 32 P10960	FAM21C	-1.59			
A 24 P455972	BC130416	-1.59			
A 23 P95353	SAPS2	-1.59			
A 24 P68079	LBA1	-1.58			
A 24 P857624	BC041417	-1.58			
A 32 P98136	KIAA1107	-1.58			
A 23 P87500	ORMDL2	-1.58			
A 23 P56933	RTN4	-1.58			
A 23 P21382	LAMB2	-1.57			
A 32 P128391	AL162073	-1.57			
A 24 P148796	MST1	-1.56			
A 23 P24157	C10orf33	-1.56			
A 23 P353478	CIITA	-1.56			
A 24 P396489	C1orf144	-1.56			
A 23 P61823	RAB24	-1.56			
A 24 P278299	ASB13	-1.56			
A 24 P343233	HLA-DRB1	-1.55			
A 23 P203463	TAF10	-1.54			
A 32 P216841	SPATA18	-1.54			
A 24 P116535	MMP15	-1.54			
A 23 P217737	ENST00000341514	-1.54			
A 24 P390055	USP30	-1.53			
A 23 P60977	LAT	-1.53			
A 23 P123454	NUDT18	-1.53			
A 23 P131646	RPIA	-1.52			
A 23 P139912	IGFBP6	-1.52			
A 23 P353097	MEGF8	-1.52			
A 23 P143600	LOC91316	-1.51			
A 23 P148556	ABCD1	-1.51			
A 32 P72611	AK097472	-1.50			
A 24 P329065	BTN3A1	-1.50			

NOTE: MDA-MB-231 cells either transfected with miR-148b precursors or negative controls (pre-miR-148b or control) were used to perform a microarray analysis (Whole Human Genome Oligo Microarray", Agilent). Up- and down-modulated protein-coding genes considering: minimum fold change (FC)=1.5; false discovery rate (FDR)=16%.

# MATERIALS AND METHODS

## **Patients and Samples**

77 frozen tumor specimens were selected from the Tumor Bank of the Department of Obstetrics and Gynecology, University of Turin. They were obtained from patients who underwent primary surgical treatment between 1988 and 2001 at a median age of 54 years (25-82). Eligibility criteria were the following: diagnosis of invasive breast cancer, all T and N stages, no distant metastasis at diagnosis (M0), complete clinical-pathological data and updated follow up. All patients were treated with radical modified mastectomy or quadrantectomy and axillary dissection plus breast irradiation. High risk node-negative and node-positive patients received adjuvant treatments (generally 6 cycles of CMF, 600 mg/m<sup>2</sup> cyclophosphamide, 40 mg/m<sup>2</sup> Metotrexate, 600 mg/m<sup>2</sup> 5-Fluorouracil) and/or 20 mg tamoxifen daily for 5 years in ER+ cases. ER and PgR status were determined by immunohistochemical stainings, patient stage distribution was assessed as prescribed by the UICC clinical staging guidelines and tumor grading was performed according to Elston and Ellis. As normal breast controls a commercial sample (RNA from Ambion, Inc., Austin, TX) and 17 frozen mammoplastic reductions (EPFL, Lausanne) were included in the screening. Appropriate ethical approval was obtained for this study.

## **Cell culture**

293T, MDA-MB-231 and 4T1 cells were from American Type Culture Collection and maintained in standard conditions: Dulbecco's Modified Eagle's Medium containing 10 mM Glutamax and 4.5 g/mL glucose (DMEM Glutamax™, GIBCO Invitrogen Life Technologies, Carlsbad, CA), supplemented with 10% heat-inactivated FCS (Seromed, GmbH), 1 mM sodium pyruvate, 25 mM HEPES pH 7.4 and 100 µg/mL gentamicin (all from GIBCO Invitrogen Life Technologies, Carlsbad, CA).

## Reagents and antibodies

miR precursors and inhibitors: Pre-miR™ miRNA Precursor Molecules-Negative Control #1, Pre-miR™ miRNA Precursor Hsa-miR-148b (PM10264), Anti-miR™ miRNA Inhibitor-Negative Control #1, Anti-miR™ miRNA Inhibitor Hsa-miR-148b (AM10264) (all from Ambion, Austin, TX). miRNA detection: TaqMan® MiRNA Assay Hsa-miR-148b ID 000471, Hsa-miR-148a ID 000470, Hsa-miR-152 ID 000475, Hsa-miR-365 ID 001020, Hsa-miR-10a ID 000387, Hsa-miR-19a ID 000395, Hsa-miR-342-3p ID 002260, Hsa-RNU44 ID 001094, U6 snRNA ID 001973 (all from Applied Biosystems, Foster City, CA). Collagen IV, Fibronectin, Laminin (from Engelbreth-Holm-Swarm murine sarcoma basement membrane) and staurosporines from Sigma Aldrich, St Louis, MO. FITC-conjugated Annexin V was provided by Boehringer Mannheim (Indianapolis, IN). Tetramethylrhodamine methyl ester (TMRM) was provided by Molecular Probes. Paclitaxel (PTX) was an ONCOTAIN trademark (Mayne Pharma, AU), Cisplatin (CDDP) was from Ebewe Italia Srl, ROMA and Doxorubicin was from Sigma Chemical Co. (St Louis, Missouri, USA). si-c-REL (Hs\_REL\_6, Hs\_REL\_4 siRNA) was purchased from QIAGEN (Stanford, CA). Primary antibodies: anti-N-RAS mAb F155, anti-hsp90 mAb F-8, anti-ROCK1 pAb H-85, anti-c-Rel mAb B-6 (all from Santa Cruz Biotechnology, Santa Cruz, CA), anti-PIK3CA #4255 and anti-PTEN pAb #9552 (Cell Signaling Technology, Danvers, MA), anti-COPZ1 pAb NBP1-00762 (Novus Biologicals, LLC, Littleton CO), anti-ITGA5 pAb RM10 kindly provided by G. Tarone (32). Secondary antibodies: goat anti-mouse IgG HRP-conjugated, goat anti-rabbit IgG HRPconjugated and donkey anti-goat IgG HRP-conjugated (all from Santa Cruz Biotechnology, Santa Cruz, CA). All antibodies were used at the producer's suggested concentrations.

## Primers

Oligonucleotides employed in this study were: cloning miR-148b, TTCATAGGCACCACTCACTTTAC and CCCTTTCCCCTTACTCTCCA ; miR-148b synthetic binding site (sensor) CTAGTCCACTGCCTGTCTGTGCCTGCTGTCGTAGGATCTACTGCCTGTCTGTGCCTGCT GTTGGACCTGACACTGCCTGTCTGTGCCTGCTGTCCCA and AGCTTGGGACAGCAGGCACAGACAGGCAGTGTCAGGTCCAACAGCAGGCACAGACAGG CAGTAGATCCTACGACAGCAGGCACAGACAGGCAGTGGA; cloning ROCK1 3'UTR, GCACTAGTGTTCCATCTTCGGACGTTGA and ATACGCGTCTTCAACAGACCATGCTCCC; cloning ITGA5 3'UTR, AACTAGTAGGCTGACCGACGACTACTG and TAACGCGTTTTTGCATACAAACTGGGAGC; cloning anti-PIK3CA p110alpha 3'UTR, AACTAGTCCTCCCTGCACTGCATTCGC and TAACGCGTCAGTGCTATGGACCATACAG; ITGA5 3'UTR mutagenesis site a, CTGGGGATCCCTCCCCCCCCACGTATTATGAAGGACCCTTGTTTA and TAAACAAGGGTCCTTCATAATACGTGGGGGGGAGGGATCCCCAG; ITGA5 3'UTR mutagenesis site b, GGGTTCTGCCTGCCAGCCGTAATTATGCTGCCCTCATCTC and GAGATGAGGGGCAGCATAATTACGGCTGGCAGGCAGAACCC; ROCK1 3'UTR deletions CATTAAGTTAACAACATATAAGAAATGTATGTTTGAATGTAAATTATTCTTAGAACACTT TC and GAAAGTGTTCTAAGAATAATTTACATTTCAAACATACATTTCTTATATGTTTGTTAACTTAA TG; qRT-PCR assays: NRAS QuantiTect Primer Assay QT00076874, CTSA QuantiTect Primer Assay QT00087381, GRB2 QuantiTect Primer Assay QT00065289, DICER1 QuantiTect Primer Assay QT00015176, BCL2 QuantiTect Primer Assay QT00025011, CXCL5 QuantiTect Primer Assay QT00203686, FDZ5 QuantiTect Primer Assay

QT00200886, CSF1 QuantiTect Primer Assay QT00035224, COPZ1 QuantiTect Primer Assay QT00087024, ESR2 QuantiTect Primer Assay QT00060641, DYRK2 QuantiTect Primer Assay QT01011073, ITGA5 QuantiTect Primer Assay QT00080871, MMP15 QuantiTect Primer Assay QT00014063, NRP1 QuantiTect Primer Assay QT00023009, ROCK1 QuantiTect Primer Assay QT00034972, MTX2 QuantiTect Primer Assay QT00084266, REL QuantiTect Primer Assay QT00052472, RRN18S QuantiTect Primer Assay QT00199367, PIK3CA QuantiTect Primer Assay QT00014861 (all from Qiagen, Stanford, CA).

### **Plasmid Construction**

Luciferase reporter vectors containing the partial 3'UTR of the indicated miR-148b target genes were generated following PCR amplification of the 3'UTR from human cDNA (by pooled RNA from SMS-CTR, RH30, RH36, RD, HT1080 and WI38 cell lines) and cloning into the Firefly Luciferase reporter pMIR-REPORT™ vector (Ambion, Austin, TX). When indicated the 3'UTRs were mutagenized at the miR-148b recognition site/s using the QuickChange Site-Directed Mutagenesis kit (Stratagene, Cedar Creek, TX) according to the manufacturer's instructions. miR-148b-sensor was obtained by annealing, purifying and cloning short oligonucleotides containing 3 perfect miR-148b binding sites into the SpeI and HindIII sites of the pMIR-REPORT™ vector.

### **RNA isolation from tissues or cells**

After surgical removal, tumor samples were macro-dissected by pathologists, quickly frozen and stored at  $-80^{\circ}\text{C}$ . Total RNA was isolated with Concert Cytoplasmic RNA Reagent (Invitrogen Life Technologies, Carlsbad, CA) from 20 to 50 mg tumor tissues, according to the

manufacturer's guidelines. Frozen tumors were placed in this reagent and homogenized using a ball mill (MM200, Retsch, Düsseldorf, Germany). The suspension was centrifuged at 14,000 x g for 5 min at 4°C, then lysed with 0.1 ml of 10% SDS followed by 0.3 ml of 5 M Sodium chloride and 0.2 ml of chloroform per ml of reagent. The lysate was centrifuged at 14,000 x g for 15 min at 4°C and the upper aqueous phase was removed and combined with 0.8 volume of isopropyl alcohol for 10 min at room temperature. The RNA was recovered by centrifugation, washed with 75% ethanol and finally dissolved in RNase-free water. Total RNA from normal samples or cells in culture was isolated with TRIzol® Reagent (Invitrogen Life Technologies, Carlsbad, CA). Each frozen sample was homogenized in the denaturing lysis solution using a homogenizer (no homogenization was used for cells) and an acid-phenol:chloroform extraction followed, according to the manufacturer's guidelines. RNA quantitation was performed using the ND-1000 spectrophotometer (Nanodrop, Wilmington, DE). The total RNA integrity and the content of miRNAs (percentage, %) in each sample were assessed by capillary electrophoresis using the Agilent Bioanalyzer 210 with the RNA 6000 Nano and the Small RNA Nano LabChips respectively (Agilent Technologies, Palo Alto, CA). Only total RNA samples with an RNA Integrity Number (RIN)  $\geq 6$  and a miRNA %  $< 30\%$  were used for miRNA microarray analysis.

### **miR and gene expression profilings**

miRNA expression profiles were carried out using the “Human microRNA Microarray kit (V2)” (Agilent Technologies, Palo Alto, CA), that allows the detection of 723 known human (miRBase v.10.1) and 76 human viral miRNAs. Each slide contains eight individual microarrays, with ~15.000 features each, including 48 negative controls, used to estimate fluorescence background and background variance. Each miRNA is targeted by 16-20 array

features, with probes of varying lengths. Total RNA (200 ng) was labeled with pCp Cy3, according to the Agilent protocol and unincorporated dyes were removed with MicroBioSpin6 columns (BioRad, Hercules, CA) (33). Probes were hybridized at 55°C for 22 hours using the Agilent's hybridization oven that is suited for bubble-mixing and microarray hybridization processes. Then, the slides were washed by Agilent Gene expression wash buffer 1 and 2 and scanned using an Agilent microarray scanner (model G2565CA) at 100% and 5% sensitivity settings. Agilent Feature Extraction software version 10.5.1.1 was used for image analysis.

Gene expression profiling was performed with the “Whole Human Genome Oligo Microarray” (Agilent Technologies, Palo Alto, CA) consisting of ~41.000 (60-mer) oligonucleotide probes, which span conserved exons across the transcripts of the targeted full-length genes. Each slide contains four individual microarrays, each with about 44.000 features. 800 ng of total RNA were labeled with “Agilent One-Color Microarray-Based Gene Expression protocol” according to the manufacturer’s instructions. The synthesized cDNA was transcribed into cRNA and labelled with cyanine 3-labelled nucleotide. Labelled cRNA was purified with RNeasy Mini columns (Qiagen, Valencia, CA). The quality of each cRNA sample was verified by total yield and specificity calculated with NanoDrop ND-1000 spectrophotometer measurements (Nanodrop, Wilmington, DE) 1.65 µg of labelled cRNA were used in each reaction and the hybridization was carried out at 65°C for 17 hours in an hybridization oven rotator (Agilent Technologies, Palo Alto, CA). The arrays were washed by Agilent Gene expression wash buffers and Stabilization and Drying Solution as suggest by the supplier. Slides were scanned on an Agilent microarray scanner and Agilent Feature Extraction software version 10.5.1.1 was used for image analysis.

### ***Statistical analysis of miR and gene expression data***

Inter-array normalization of expression levels was performed with cyclic Lowess for miRNA experiments and with quantile for gene expression profilings (34) in order to correct possible experimental distortions. Normalization function was applied to expression data of all experiments and then values of spot replicates within arrays were averaged. Furthermore, Feature Extraction Software provides spot quality measures in order to evaluate the quality and the reliability of the hybridization. In particular, flag "glsFound" (set to 1 if the spot has an intensity value significantly different from the local background, 0 otherwise) was used to filter out unreliable probes: flag equal to 0 will be noted as "not available (NA)". So, in order to make more robust and unbiased statistical analysis, probes with a high proportion of "NA" values were removed from the dataset. We decided to use the 40% of NA as threshold in the filtering process obtaining a total of 237 available human miRs. Principal component analysis, cluster analysis and profile similarity searches were performed with Multi Experiment Viewer version 4.5.1 (TMev ) that is part of the TM4 Microarray Software Suite (35). To perform differential gene expression analysis the level of each miR was calculated as  $\log_2$  of tumor sample / mammaplastic reduction median. The identification of differentially expressed genes and miRs was performed with two class Significance Analysis of Microarray (SAM) program (36) with default settings. SAM uses a permutation-based multiple testing algorithm and identifies significant genes and miRNA with variable false-discovery rates (FDR). This can be manually adjusted to include a reasonable number of candidate genes with acceptable and well defined error probabilities. All showed heat maps were obtained by TMeV software using an unsupervised two-dimensional hierarchical clustering approach with average linkage method and Pearson correlation.

## qRT-PCR for miR or mRNA detection

miRNA microarray result validations and miR detection for *in vitro* experiments were performed by the TaqMan<sup>®</sup> MiRNA Assay kit (Applied Biosystems, Foster City, CA) that incorporates a target-specific stem-loop reverse transcription primer to provide specificity for the mature miRNA target. The RT primer/mature miRNA-chimera extends to the 5' end of the miRNA. The resulting longer RT amplicon presents a template amenable to standard real-time PCR using TaqMan Assays (37). In brief, each RT reaction (15  $\mu$ l) contained 10 ng of total purified RNA, 5X stem-loops RT primer, 1X RT buffer, 0.25 mM each of dNTPs, 50U MultiScribe<sup>™</sup> reverse transcriptase and 3.8U RNase inhibitor. The reactions were incubated in a Thermal Cycler (Applied Biosystems, Foster City, CA) in 0.2 ml PCR tubes for 30 min at 16°C, 30 min at 42°C, followed by 5 min at 85°C, and then held at 4°C. The resulting cDNA was semiquantitatively amplified in 40 cycles on an ABI 7500 Real-Time PCR System, using TaqMan Universal PCR Master Mix and Taqman MicroRNA Assays. For each real-time PCR reaction three replicates of each sample and endogenous control were amplified. For mRNA detection, 1  $\mu$ g of DNase-treated RNA (DNA-free<sup>™</sup> kit, Ambion, Austin, TX) was retrotranscribed with RETROscript<sup>™</sup> reagents (Ambion, Austin, TX) and qRT-PCRs were carried out using gene-specific primers, by a 7900HT Fast Real Time PCR System (standard settings). As endogenous normalizers the expression of the RNU44 small nucleolar RNA or of 18s ribosomal RNA were chosen for miR or mRNA detection, respectively. The relative expression levels between samples were calculated using the comparative delta CT (threshold cycle number) method ( $2^{-\Delta\Delta CT}$ ) (38). In the case of tumor samples, the median expression for miR or mRNA was used across samples as calibrator, while for cell lines the control sample was the reference point (38).

## **Survival Statistics**

Survival association analyses were performed using the SPSS 13.0 statistical software (SPSS Inc, Chicago, Ill). The ROC (receiver operating characteristic) method was used to categorize samples according to miR or mRNA expression above or below median expression across samples. Kaplan-Meier survival curves were used to estimate time-to-event models in the presence of censored cases. Risk differences between the two groups were assessed using the Mantel-Haenszel Log-rank test. Survival analysis was carried out in both univariate and multivariate setting using Cox's proportional hazard model. Variables that were significant at univariate level ( $p < .05$ ) were considered to build multivariate model.

## **Analysis of human breast cancer data sets**

Blenkiron miR expression data and Blenkiron sample phenodata (28) were obtained from GSE7842 GEO record and each ref ID was mapped to the correct miR according to the GPL5173 table.

The evaluation of the differentially expressed miR classification power was performed by Weka software (Version 3.4.8 (39)) using the Support Vector Machine (SMO) and the partial decision trees algorithms to train and classify samples. In particular, either according to lymph node either according to miR expression, our samples and samples from Blenkiron et al. dataset were divided by chance in two groups; one group was used to train the classification algorithm and the other to test the learned method.

## **Target Prediction and Pathway Analysis**

The miRecords System (<http://mirecords.biolead.org>) was used to predict miR targets; at least three different algorithms were considered.

The Ingenuity Pathways Knowledge Base ([www.ingenuity.com](http://www.ingenuity.com)) is currently the world's largest database of knowledge on biological networks, with annotations organized by experts. We exploited this database to look for enrichments in specific pathways among the relapse (or other categories) associated miR putative targets.

### **Transient transfections of pre-miRs, anti-miRs or siRNAs**

To obtain transient anti-miR, pre-miR, or siRNA expression, cells were plated in 6-well plates at 30-50% confluency and transfected 24h later using RNAiFect (QIAGEN, Stanford, CA) reagent, according to manufacturer's instructions, with 75 nM anti-miR, 75 nM pre-miR or 200 nM siRNA. Cells were tested for miR overexpression/knockdown or gene knockdown 24h, 48h or 72h later.

### **Invasion assays**

To measure invasion  $5 \times 10^4$  MDA-MB-231 or 4T1 cells were seeded in serum-free media respectively in the upper chambers of cell culture inserts (transwells) with 8.0  $\mu\text{m}$  pore size membrane (24-well format, Becton Dickinson, NJ) precoated with 10  $\mu\text{g}/\text{mL}$  fibronectin, or in the upper chambers of BioCoat™ Matrigel Invasion Chambers with 8.0  $\mu\text{m}$  pore size membrane (Becton Dickinson, NJ). The lower chambers were filled with complete growth media. After 18-20h, the migrated cells present on the lower side of the membrane were fixed with methanol, stained with haematoxylin and eosin (Diff-Quik, Medion Diagnostics, Dudingen, CH) and photographed using an Olympus IX70 microscope (40). Invasion was evaluated by measuring the area occupied by migrated cells using the ImageJ software (<http://rsbweb.nih.gov/ij/>).

### **Adhesion assays**

To test adhesion,  $5 \times 10^4$  cells/well were seeded onto 5  $\mu\text{g/mL}$  collagen IV or 10  $\mu\text{g/mL}$  fibronectin or 5  $\mu\text{g/mL}$  laminin (all from Sigma-Aldrich, St Louis, MO) precoated 96-well plates, for 1h at 37°C. Cells were then washed thoroughly to remove non-adherent cells, fixed with methanol and stained with haematoxylin and eosin (Diff-Quik, Medion Diagnostics, Dudingen, CH). Wells were photographed using Olympus IX70 microscope and the area occupied by the adherent cell was measured by using the ImageJ software (<http://rsbweb.nih.gov/ij/>) (40).

### **Proliferation assays**

$5 \times 10^3$  cells/well were plated in 96-well plates in complete medium and starved for 24h. Complete medium was then added and cells were allowed to grow for 1, 2, 3, 4 days, fixed with 2.5% glutaraldehyde and stained with 0.1% crystal violet. The dye was solubilised using 10% acetic acid and optical density measured directly in plates using a Microplate Reader Mithras LB940 (Berthold Technologies, GmbH) at 570 nm wavelength (41).

### **Anchorage-independent growth assays**

$5 \times 10^4$  cells were resuspended in 8 mL of complete DMEM containing 0.45% Difco Noble Agar (Becton Dickinson, NJ) and plated in 6 cm bacterial dishes. Medium was changed every 3 days. 30 days later the dishes were stained with nitroblue tetrazolium (Sigma-Aldrich, St Louis, MO), photographed with Nikon SMZ1000 stereomicroscope and colonies were counted using the ImageJ software (<http://rsbweb.nih.gov/ij/>) (42).

### **Anoikis analysis**

Cells were plated on a 2% agarose pad in serum-free medium for 48h, collected, washed in PBS buffer, resuspended in 10 mM Hepes, 150 mM NaCl, 5 mM CaCl<sub>2</sub> buffer containing FITCconjugated Annexin-V (Bender MedSystems, GmbH) and 200 nM tetramethyl-rhodamine-methyl-7ester (TMRM, Molecular Probes, Invitrogen, CA) and incubated at 37°C for 15 minutes. Flow cytometry analysis of apoptosis was carried out by using a FACSCalibur flow cytometer (Becton Dickinson, NJ). Data acquisition was performed using CellQuest software (Becton Dickinson, NJ) and data analysis with WinMDI software (version 2.8, Scripps Institute, CA). Results were displayed in bidimensional plots, with gates indicating the percentages of healthy and apoptotic populations (43).

### **Apoptosis assays**

In order to trigger apoptosis, 72 h after miR transfections, cells were plated at 45000/cm<sup>2</sup> density, grown in complete medium with or without drugs for 24 or 48h; Paclitaxel (PTX) 5μM, Doxorubicin (DOXO) 1μM and Cisplatin (CDDP) 100μM. After apoptosis induction cells were washed once in phosphate-buffered saline (PBS) and detached by trypsinization. Labeling and analysis was performed as in Anoikis analysis.

### **Luciferase assays**

15x10<sup>4</sup> cells were cotransfected with 50 ng of the pMIR REPORT™ (Ambion, Austin, TX) Firefly Luciferase constructs containing the 3'UTRs of the indicated miR-148b potential target genes and 20 ng of pRL-TK Renilla Luciferase normalization control (Promega, Madison, WI), using Lipofectamine™2000 (Invitrogen Life Technologies, Carlsbad CA). Lysates were

collected 48h after transfection and Firefly and Renilla Luciferase activities were measured with a Dual- Luciferase Reporter System (Promega, Madison, WI).

### **Protein preparation and Immunoblotting**

Total protein extracts were obtained using a boiling buffer containing 0.125 M Tris/HCl, pH 6.8 and 2.5% sodium dodecyl sulphate (SDS). 25 µg proteins were separated by SDS polyacrylamide gel electrophoresis (PAGE) and electroblotted on to polyvinylidene fluoride (PVDF) membranes (Bio-Rad, Hercules, CA). Membranes were blocked in 5% BSA Tris buffered saline (TBS)-Tween buffer (137 mM NaCl, 20 mM Tris/HCl, pH 7.6, 0.1% Tween-20) for 1h at 42°C, then incubated with appropriate primary and secondary antibodies in 1% BSA TBS-Tween buffer, respectively overnight at 4°C and for 1h at room temperature and visualized by enhanced chemiluminescence (ECL®, Amersham Biosciences, Pisactaway, NJ).

### **Statistical analyses**

Unless otherwise noted, data are presented as mean ± Standard Error of the Mean (SEM) and two tailed Student's t test was used for comparisons. n.s. indicates a not statistically significant *p*-value.

# DISCUSSION

We analyzed the expression of over 700 miRNAs in human breast cancer samples and identified a miRNA signature able to classify tumor samples according to relapse behaviour in two different breast cancer patient cohorts. Considering the biological functions of the putative targets related to the 16 miRNA signature we observed a strong correlation with cancer biology and tumor progression. When we evaluated the signalling coordinated by the identified small RNAs, one miRNA in particular, was able to coordinate the highest number of pathways, miR-148b, downmodulated in poor prognosis tumors. Based on these predictions, we hypothesized that miR-148b played a major role in breast tumorigenesis, therefore we analyzed its biological relevance in details. In a model of basal like breast cancer, we demonstrated that miR-148b coordinates *in vitro* cell adhesion proliferation, anchorage independent cell growth, anoikis survival, invasion and resistance to chemotherapeutical agents. Finally, we proved that miR-148b directly down-regulates genes involved in the integrin pathway.

Our biological results obtained for miR-148b suggest a metastasis-suppressing role for miR-148b. However, its influence on cell growth is not totally clear, at this point. The fact that miR-148b overexpression leads to increased cell proliferation in cell cycle and plate cell culture experiments but reduces anchorage independent growth could suggest a specific influence on stem cells by miR-148b that needs further investigations. In addition, the reduction of cell movement observed following miR-148b overexpression could suggest that this small RNA coordinates tumorigenesis and metastasis formation in two distinct manners. Overall, generally, even if tumor formation is a pre-requisite for progression, metastasis can be considered an independent secondary step, consequent to the activation or repression of a selective and rate-limiting cascade of specific genes (44). Not surprisingly, pleiotropical functions were already demonstrated for other miRNAs (28, 45), as the biological effects of

any miRNA depend on a fine-tuned balance between the modulation of its targets and the molecular context in which these modulations occurs.

Our *in vitro* experiments modelled only single steps involved in tumorigenesis and metastasis formation, the general context was not analyzed. When we investigating the role of miR-148b in proliferation, in an adherent bi-dimensional context, we envisaged an oncogenic role for miR-148b since overexpression was promoting cell growth. In this context miR-148b putative targets, BCL2 and CDK6, were upregulated at the mRNA level, suggesting an additional promoting effect of miR-148b on cell growth (46, 47). However, in absence of adhesion, miR-148b overexpressing cells underwent apoptosis and did not growth.

In the patients, in an *in vivo* context, miR-148b provides a favourable prognosis. This could be related to different actions of miR-148b, impairing the metastatic cascade at multiple levels. In particular, it could decrease survival in the blood circulation by increasing anoikis apoptosis and inhibiting tumor invasion, in fact, in presence of high levels of miR-148b, anoikis is increased in plates and invasion is reduced in transwell assays. However, miR-148 could also have a major role in impairing therapy resistance since it boosts apoptosis induced by chemotherapeutical drugs *in vitro*. miR-148b could even exert this function by increasing cellular growth, as this effect enhances sensitivity to chemotherapy (48).

Expression of certain miR-148b effectors correlates with both miR-148b antimetastatic function and drug responsiveness. We demonstrated that ITGA5 is downmodulated by miR-148b at the mRNA and protein levels and that it is a direct target of miR-148b. Many literature evidences show that Integrin  $\alpha 5$  coordinates numerous of the biological functions in which miR-148b is involved, following ITGA5 formation of heterodimers with integrine  $\beta 1$  and binding to fibronectin. In particular, elevated levels and activity of  $\alpha 5\beta 1$  have been implicated in drug-resistance in breast carcinoma cells (49). In fact, Inhibition of  $\alpha 5\beta 1$ /fibronectin

interactions promotes apoptosis in malignant cells and enhances the apoptotic effects of radiations. In addition, an analysis of gene expression array data from breast cancer patients correlates high *levels* of  $\alpha 5$ -integrin expression with decreased survival (50). Moreover integrin  $\alpha 5$  serves as a key mediator of Src and ErbB2-survival signaling in low adhesion states (51).

The integrin-mediated apoptosis is linked to another miR-148b downmodulated target, ROCK1. There is increasing evidence that ROCK-mediated focal adhesion and integrin activation are involved in cell survival. Perturbations of the actin cytoskeleton integrity via ROCK inhibition can initiate events that commit a cell to apoptosis (52). Moreover, ROCK signalling promotes breast cancer metastasis (53) and ROCK1 expression, in particular, is much higher in primary breast cancers that give rise to metastases than in tumors that do not metastasize (54).

Literature provides evidences of breast cancer involvement also for p110 $\alpha$ , another miR-148b downmodulated target. Preclinical studies have found that PIK3CA activity induces mammary tumorigenesis and angiogenesis (55). In addition, activation of the PI3K/Akt pathway coupled with PTEN loss, has been associated with resistance to endocrine therapy and to anti-HER2 treatments, trastuzumab and lapatinib (56, 57). Due to that a number of drugs targeting the PI3K/Akt signalling pathway have already been developed and found to block tumor growth not only by targeting tumor cells but also via their effects on tumor vasculature (58). Their effect as monotherapy is low, but some data of combination with other drugs are promising (59).

NRAS downmodulated at the protein level by miR-148b has oncogenic role in many cancers and activating mutations of the RAS family occur in approximately a third of all human cancers. Suppression of oncogenic NRAS in melanoma cell lines resulted in

increased apoptosis. Furthermore, N-Ras signaling pathway analysis showed decreased phosphorylation of extracellular signal-regulated kinase (ERK) and Akt, and reduced expression of NF- $\kappa$ B and cyclin D1 in (60).

According to literature data these miR-148b effectors could sustain breast tumor growth, and metastatic formation and promote chemotherapy resistance as single players. However, they are also involved in a coordinated pathway linked to integrins signalling regulating cellular growth, apoptosis and cellular movement (Figure 11). Other miRs already involved in the breast cancer metastatic process are regulators of the same players or of other genes involved in this pathway. In particular, among the metastasis suppressors, miR-31 was found to inhibit expression of ITGA5 and RHOA, a ROCK activator (61), whereas miR-146 a and b have been found to downmodulate EGF receptor (62) and ROCK1 (63). On the contrary, miR-10b up-regulation leads to increased expression of RHOC (64).

Our findings, together with the literature data mentioned above, suggest a particular tight and redundant regulation of the integrin pathways suggesting a specific involvement in breast cancer progression. Thanks to that we can assume that the assessment of integrin signalling molecules together with the measure of related miRs, such as miR-148b, miR-31 and miR146a/b could be useful to estimate breast cancer prognosis. In addition, miR-148b expression could have an important impact on the outcome of breast cancer treatment, in particular for chemotherapy. miR-148b role in overcoming therapy resistance needs to be investigated more in details together with the consequent involvement of integrin signalling.

Of particular interest in the integrin signaling context are also the results we obtained analyzing association with survival of the miR-148b host gene, COPZ1. This gene encodes a protein involved in the vesicular trafficking clatrin independent. The COPZ proteins have a central role in this process, creating a sorting domain on the membrane into which cargo

proteins, destined to return to the endoplasmic reticulum (ER), concentrate (65). This kind of secretory transport is involved in EGF receptor recycling and in particular is linked to the intracellular receptor signalling turn-off (66). As we showed, COPZ1 high expression correlates with good prognosis, providing again a link with mechanisms of integrin signalling downmodulation.

Considering the increasing evidence of cooperation between transcription factors and miRs regulating the same targets (25), we explored a database of gene regulatory circuits (CIRCUITSDB,(26)). In this database are collected gene regulation network characteristic motifs termed Mixed Feed Forward Loop in which a transcription factors regulate a target directly or via regulation of its miR controller. We found that the c-REL transcription factor, member of the NFkB family, controls ITGA5 directly and via miR-148b, and in particular we demonstrated that c-REL negatively regulates miR-148b. This influence on miR-148b acquires particular significance by the fact that miR-146a/b-mediated NFkB downmodulation, together with IRAK1 and TRAF6 targeting, inhibit invasion and migration of breast cancer cells (62). Interestingly, considering therapeutic repercussions, Cioce and colleagues, in a drug-screen assay, identified a total of 26 compounds able to kill specifically a MCF7 cell population enriched in cancer stem cell, all interfering with NFkB signaling (67). This evidence coupled with miR-148b effects in chemotherapy provides a remarkable insight into c-REL/miR-148b ITGA5 regulation and cancer stem cell targeting.

The analysis of this circuit has to be completed studying the direct c-REL regulation of ITGA5. The direction of this control will give important information about the kind and time of regulatory response.

In conclusion, in our study we explored the function of a novel miR, miR-148b, correlated with breast cancer behaviour. We were able to connect it with a regulatory network

in which ITGA5 is an important player with significant action in the metastatic process and in therapy response. Rescuing experiments to link directly ITGA5 to miR-148b biological functions have to be done, in order to test the link between miR-148b and the ITGA5 pathway for *in vivo* therapeutic targeting.

# ACKNOWLEDGEMENTS

This work was supported by grants from the University of Torino (Local Research Funding 2007/DT, 2008/DT), Regione Piemonte Ricerca Scientifica Applicata (CIPE2004/DT) and Compagnia di San Paolo, Torino and I am fellow of the Regione Piemonte.

I would like to thank Cathrin Brisken and Sara Cabodi for reviewing this manuscript, Daniela Taverna that greatly encouraged and supported my scientific growth and Michele De Bortoli that allowed my first experiences in research field. A particular thank also to Francesca Orso, to the other people in the lab and to Cristiano De Pittà and Matteo Zampini for help in 3'UTR cloning.

Finally I dedicate this work to my precious family.

# BIBLIOGRAPHY

1. Jemal A, Siegel R, Ward E, Hao Y, Xu J, Thun MJ. Cancer statistics, 2009. *CA Cancer J Clin* 2009;59:225-49.
2. Jemal A, Siegel R, Xu J, Ward E. Cancer statistics, 2010. *CA Cancer J Clin*;60:277-300.
3. Dunnwald LK, Rossing MA, Li CI. Hormone receptor status, tumor characteristics, and prognosis: a prospective cohort of breast cancer patients. *Breast Cancer Res* 2007;9:R6.
4. van 't Veer LJ, Dai H, van de Vijver MJ, et al. Gene expression profiling predicts clinical outcome of breast cancer. *Nature* 2002;415:530-6.
5. Effects of chemotherapy and hormonal therapy for early breast cancer on recurrence and 15-year survival: an overview of the randomised trials. *Lancet* 2005;365:1687-717.
6. Berry DA, Cirincione C, Henderson IC, et al. Estrogen-receptor status and outcomes of modern chemotherapy for patients with node-positive breast cancer. *JAMA* 2006;295:1658-67.
7. Harris L, Fritsche H, Mennel R, et al. American Society of Clinical Oncology 2007 update of recommendations for the use of tumor markers in breast cancer. *J Clin Oncol* 2007;25:5287-312.
8. Harari D, Yarden Y. Molecular mechanisms underlying ErbB2/HER2 action in breast cancer. *Oncogene* 2000;19:6102-14.
9. Press MF, Pike MC, Chazin VR, et al. Her-2/neu expression in node-negative breast cancer: direct tissue quantitation by computerized image analysis and association of overexpression with increased risk of recurrent disease. *Cancer Res* 1993;53:4960-70.
10. Piccart-Gebhart MJ, Procter M, Leyland-Jones B, et al. Trastuzumab after adjuvant chemotherapy in HER2-positive breast cancer. *N Engl J Med* 2005;353:1659-72.
11. Goldhirsch A, Ingle JN, Gelber RD, Coates AS, Thurlimann B, Senn HJ. Thresholds for therapies: highlights of the St Gallen International Expert Consensus on the primary therapy of early breast cancer 2009. *Ann Oncol* 2009;20:1319-29.
12. Eifel P, Axelson JA, Costa J, et al. National Institutes of Health Consensus Development Conference Statement: adjuvant therapy for breast cancer, November 1-3, 2000. *J Natl Cancer Inst* 2001;93:979-89.
13. Galea MH, Blamey RW, Elston CE, Ellis IO. The Nottingham Prognostic Index in primary breast cancer. *Breast Cancer Res Treat* 1992;22:207-19.
14. Sorlie T, Perou CM, Tibshirani R, et al. Gene expression patterns of breast carcinomas distinguish tumor subclasses with clinical implications. *Proc Natl Acad Sci U S A* 2001;98:10869-74.
15. Sotiriou C, Piccart MJ. Taking gene-expression profiling to the clinic: when will molecular signatures become relevant to patient care? *Nat Rev Cancer* 2007;7:545-53.
16. Fan C, Oh DS, Wessels L, et al. Concordance among gene-expression-based predictors for breast cancer. *N Engl J Med* 2006;355:560-9.
17. Paik S, Shak S, Tang G, et al. A multigene assay to predict recurrence of tamoxifen-treated, node-negative breast cancer. *N Engl J Med* 2004;351:2817-26.
18. Sparano JA, Paik S. Development of the 21-gene assay and its application in clinical practice and clinical trials. *J Clin Oncol* 2008;26:721-8.
19. van de Vijver MJ, He YD, van't Veer LJ, et al. A gene-expression signature as a predictor of survival in breast cancer. *N Engl J Med* 2002;347:1999-2009.
20. Cardoso F, Van't Veer L, Rutgers E, Loi S, Mook S, Piccart-Gebhart MJ. Clinical application of the 70-gene profile: the MINDACT trial. *J Clin Oncol* 2008;26:729-35.
21. Achard P, Herr A, Baulcombe DC, Harberd NP. Modulation of floral development by a gibberellin-regulated microRNA. *Development* 2004;131:3357-65.
22. Kim VN. MicroRNA biogenesis: coordinated cropping and dicing. *Nat Rev Mol Cell Biol* 2005;6:376-85.

23. Carthew RW, Sontheimer EJ. Origins and Mechanisms of miRNAs and siRNAs. *Cell* 2009;136:642-55.
24. Greene SB, Gunaratne PH, Hammond SM, Rosen JM. A putative role for microRNA-205 in mammary epithelial cell progenitors. *J Cell Sci*;123:606-18.
25. Re A, Cora D, Taverna D, Caselle M. Genome-wide survey of microRNA-transcription factor feed-forward regulatory circuits in human. *Mol Biosyst* 2009;5:854-67.
26. Friard O, Re A, Taverna D, De Bortoli M, Cora D. CircuitsDB: a database of mixed microRNA/transcription factor feed-forward regulatory circuits in human and mouse. *BMC Bioinformatics*;11:435.
27. Lu J, Getz G, Miska EA, et al. MicroRNA expression profiles classify human cancers. *Nature* 2005;435:834-8.
28. Blenkiron C, Goldstein LD, Thorne NP, et al. MicroRNA expression profiling of human breast cancer identifies new markers of tumor subtype. *Genome Biol* 2007;8:R214.
29. Dumont N, Tlsty TD. Reflections on miR-ing effects in metastasis. *Cancer Cell* 2009;16:3-4.
30. Hurst DR, Edmonds MD, Welch DR. Metastamir: the field of metastasis-regulatory microRNA is spreading. *Cancer Res* 2009;69:7495-8.
31. Shi M, Liu D, Duan H, Shen B, Guo N. Metastasis-related miRNAs, active players in breast cancer invasion, and metastasis. *Cancer Metastasis Rev*;29:785-99.
32. Tarone G, Russo MA, Hirsch E, et al. Expression of beta 1 integrin complexes on the surface of unfertilized mouse oocyte. *Development* 1993;117:1369-75.
33. Wang H, Ach RA, Curry B. Direct and sensitive miRNA profiling from low-input total RNA. *RNA* 2007;13:151-9.
34. Bolstad BM, Irizarry RA, Astrand M, Speed TP. A comparison of normalization methods for high density oligonucleotide array data based on variance and bias. *Bioinformatics* 2003;19:185-93.
35. Saeed AI, Bhagabati NK, Braisted JC, et al. TM4 microarray software suite. *Methods Enzymol* 2006;411:134-93.
36. Tibshirani R, Hastie T, Narasimhan B, Chu G. Diagnosis of multiple cancer types by shrunken centroids of gene expression. *Proc Natl Acad Sci U S A* 2002;99:6567-72.
37. Chen C, Ridzon DA, Broomer AJ, et al. Real-time quantification of microRNAs by stem-loop RT-PCR. *Nucleic Acids Res* 2005;33:e179.
38. Bookout AL, Mangelsdorf DJ. Quantitative real-time PCR protocol for analysis of nuclear receptor signaling pathways. *Nucl Recept Signal* 2003;1:e012.
39. Frank E, Hall M, Trigg L, Holmes G, Witten IH. Data mining in bioinformatics using Weka. *Bioinformatics (Oxford, England)* 2004;20:2479-81.
40. Orso F, Penna E, Cimino D, et al. AP-2alpha and AP-2gamma regulate tumor progression via specific genetic programs. *FASEB J* 2008;22:2702-14.
41. Kueng W, Silber E, Eppenberger U. Quantification of cells cultured on 96-well plates. *Anal Biochem* 1989;182:16-9.
42. Hynes NE, Taverna D, Harwerth IM, et al. Epidermal growth factor receptor, but not c-erbB-2, activation prevents lactogenic hormone induction of the beta-casein gene in mouse mammary epithelial cells. *Mol Cell Biol* 1990;10:4027-34.
43. Rasola A, Geuna M. A flow cytometry assay simultaneously detects independent apoptotic parameters. *Cytometry* 2001;45:151-7.
44. Ma L, Weinberg RA. Micromanagers of malignancy: role of microRNAs in regulating metastasis. *Trends Genet* 2008;24:448-56.
45. Tavazoie SF, Alarcon C, Oskarsson T, et al. Endogenous human microRNAs that suppress breast cancer metastasis. *Nature* 2008;451:147-52.

46. Ruiz C, Seibt S, Al Kuraya K, et al. Tissue microarrays for comparing molecular features with proliferation activity in breast cancer. *Int J Cancer* 2006;118:2190-4.
47. Finn RS, Dering J, Conklin D, et al. PD 0332991, a selective cyclin D kinase 4/6 inhibitor, preferentially inhibits proliferation of luminal estrogen receptor-positive human breast cancer cell lines in vitro. *Breast Cancer Res* 2009;11:R77.
48. Rosen LS, Ashurst HL, Chap L. Targeting signal transduction pathways in metastatic breast cancer: a comprehensive review. *Oncologist*;15:216-35.
49. Nista A, Leonetti C, Bernardini G, Mattioni M, Santoni A. Functional role of alpha4beta1 and alpha5beta1 integrin fibronectin receptors expressed on adriamycin-resistant MCF-7 human mammary carcinoma cells. *Int J Cancer* 1997;72:133-41.
50. Nam JM, Onodera Y, Bissell MJ, Park CC. Breast cancer cells in three-dimensional culture display an enhanced radioresponse after coordinate targeting of integrin alpha5beta1 and fibronectin. *Cancer Res*;70:5238-48.
51. Haenssen KK, Caldwell SA, Shahriari KS, et al. ErbB2 requires integrin alpha5 for anoikis resistance via Src regulation of receptor activity in human mammary epithelial cells. *J Cell Sci*;123:1373-82.
52. Shi J, Wei L. Rho kinase in the regulation of cell death and survival. *Arch Immunol Ther Exp (Warsz)* 2007;55:61-75.
53. Liu S, Goldstein RH, Scepansky EM, Rosenblatt M. Inhibition of rho-associated kinase signaling prevents breast cancer metastasis to human bone. *Cancer Res* 2009;69:8742-51.
54. Lane J, Martin TA, Watkins G, Mansel RE, Jiang WG. The expression and prognostic value of ROCK I and ROCK II and their role in human breast cancer. *Int J Oncol* 2008;33:585-93.
55. Renner O, Blanco-Aparicio C, Grassow M, Canamero M, Leal JF, Carnero A. Activation of phosphatidylinositol 3-kinase by membrane localization of p110alpha predisposes mammary glands to neoplastic transformation. *Cancer Res* 2008;68:9643-53.
56. Miller TW, Hennessy BT, Gonzalez-Angulo AM, et al. Hyperactivation of phosphatidylinositol-3 kinase promotes escape from hormone dependence in estrogen receptor-positive human breast cancer. *J Clin Invest*;120:2406-13.
57. Eichhorn PJ, Gili M, Scaltriti M, et al. Phosphatidylinositol 3-kinase hyperactivation results in lapatinib resistance that is reversed by the mTOR/phosphatidylinositol 3-kinase inhibitor NVP-BEZ235. *Cancer Res* 2008;68:9221-30.
58. Schnell CR, Stauffer F, Allegrini PR, et al. Effects of the dual phosphatidylinositol 3-kinase/mammalian target of rapamycin inhibitor NVP-BEZ235 on the tumor vasculature: implications for clinical imaging. *Cancer Res* 2008;68:6598-607.
59. Courtney KD, Corcoran RB, Engelman JA. The PI3K pathway as drug target in human cancer. *J Clin Oncol*;28:1075-83.
60. Eskandarpour M, Kiaii S, Zhu C, Castro J, Sakko AJ, Hansson J. Suppression of oncogenic NRAS by RNA interference induces apoptosis of human melanoma cells. *Int J Cancer* 2005;115:65-73.
61. Valastyan S, Chang A, Benaich N, Reinhardt F, Weinberg RA. Concurrent suppression of integrin alpha5, radixin, and RhoA phenocopies the effects of miR-31 on metastasis. *Cancer Res*;70:5147-54.
62. Hurst DR, Edmonds MD, Scott GK, Benz CC, Vaidya KS, Welch DR. Breast cancer metastasis suppressor 1 up-regulates miR-146, which suppresses breast cancer metastasis. *Cancer Res* 2009;69:1279-83.
63. Lin SL, Chiang A, Chang D, Ying SY. Loss of mir-146a function in hormone-refractory prostate cancer. *RNA* 2008;14:417-24.

64. Ma L, Teruya-Feldstein J, Weinberg RA. Tumour invasion and metastasis initiated by microRNA-10b in breast cancer. *Nature* 2007;449:682-8.
65. Lippincott-Schwartz J, Liu W. Insights into COPI coat assembly and function in living cells. *Trends Cell Biol* 2006;16:e1-4.
66. Sigismund S, Argenzio E, Tosoni D, Cavallaro E, Polo S, Di Fiore PP. Clathrin-mediated internalization is essential for sustained EGFR signaling but dispensable for degradation. *Dev Cell* 2008;15:209-19.
67. Cioce M, Gherardi S, Viglietto G, et al. Mammosphere-forming cells from breast cancer cell lines as a tool for the identification of CSC-like- and early progenitor-targeting drugs. *Cell Cycle*;9:2878-87.

# REVIEWER COMMENTS

**Sara Cabodi**

[sara.cabodi@unito.it](mailto:sara.cabodi@unito.it)

Researcher at the University of Turin, Department of Genetics, Biology and Biochemistry, Molecular Biotechnology Center, Via Nizza, 52, Turin.

To whom it may concern,

The aim of Daniela Cimino' PhD Thesis is to address the relevance of a 16 miRNA relapse-signature to predict survival of breast cancer patients and to identify the signalling pathways in which these miRNAs are involved. She identified miR-148b as a crucial regulator of breast tumorigenesis and demonstrated that miR-148b promotes in vitro cell adhesion, cell proliferation and survival in a model of basal like breast cancer. Moreover, miR-148b impaired invasion and resistance to chemotherapeutical agents. Daniela was able to connect miR-148b expression with a regulatory network in which Integrin alpha 5 is an important player acting in the metastatic process and in the response to therapy.

I really enjoyed reading Daniela's Thesis. The project of the Thesis is very innovative, the Thesis very well written and all the sections are described in a very clear and detailed manner. The results produced by Daniela are very interesting and well supported by the huge amount of data presented both in the Results and in the Supplementary section. Her Thesis provides new evidences on the existence of a miR signature that can be used to stratify breast cancer patients and to predict their survival. It describes also a very intriguing network that can have implications in the therapy response. In conclusion, I think that this Thesis adds an important piece of knowledge for understanding breast cancer progression.

Yours sincerely, Sara Cabodi

**Catherine Brisken**

[cathrin.brisken@isrec.ch](mailto:cathrin.brisken@isrec.ch)

Associate scientist in the NCCR Molecular Oncology program.

Swiss Institute for Experimental Cancer Research, National Center of Competence in Research in  
Molecular Oncology

155 Chemin des Boveresses, CH-1066 Epalinges/Lausanne, Switzerland

**SCHOOL OF LIFE SCIENCES– FACULTE DES SCIENCES DE LA VIE**  
**Swiss institute for experimental cancer research - ISREC**  
**Institut suisse de recherche expérimentale sur le cancer - ISREC**



**ÉCOLE POLYTECHNIQUE  
FÉDÉRALE DE LAUSANNE**

EPFL SV-ISREC  
SV2.832 Station 19  
CH-1015 Lausanne, Switzerland

Téléphone : +41 (0)21 692 58 58  
Fax : +41 (0)21 652 69 33  
Site web : <http://isrec.epfl.ch>

**Prof. Cathrin BRISKEN**

*Phone: 021 693 07 81*

*Sec. Lisa Cepeda: 021 693 07 62*

*Fax: 021 693 07 40*

E-mail: [cathrin.brisken@epfl.ch](mailto:cathrin.brisken@epfl.ch)

**Prof. Daniela Taverna, PhD**

Molecular Biotechnology Center

Dept. Oncological Sciences

University of Turin Via Nizza, 52

10126 Torino

Italy

Phone: +39 011 670 6497

Fax: +39 011 670 6432

Lausanne, December 10th 2010

Report of the PhD thesis entitled:

**“miR-148b is a major coordinator in a Relapse-associated  
miR signature in Breast Tumors ”**

Presented by

**Madame Daniela CIMINO,**

**UNIVERSITA' DEGLI STUDI DI TORINO**

*Department of Oncological Sciences*

**Ph.D. in Complex Systems applied to Post-Genomic Biology**

XXIII Cycle

Dear Sir/Madam,

The present thesis is a very complex and comprehensive piece of work and is very clear, well structured and well written. The introduction reviews nicely the field and adequately quotes relevant publications. The candidate used a wide spectrum of experimental approaches and acquired an impressive amount of data. The data are very well presented and clear.

The candidate uses 77 ductal carcinomas to identify miR that are differentially expressed between tumors that relapsed and that did not in the 72 months ensuing tumor removal. She identifies

16 miRs among which miR-148b stands out as major coordinator. An impressive amount of bioinformatic and statistical analyses are performed. Ms Cimino then proceeded to analyze the biological function of miR-148 using different breast cancer cell lines and links it to the cell adhesion gene ITGA5 and the transcription factor c-rel. Interestingly, expression of the mir-148b host gene COPZ1 correlates with mir-148b expression

Taken together this thesis is an impressive and thorough piece of work and I accept it without reservations.

#### Points/Questions:

1. 16 miRs are identified that distinguish patients with relapse within 72 months from those without. Differentially expressed miRs were also identified when ER positive versus ER negative carcinomas were compared. Generally, hormone receptor negative tumors (in particular triple negative ones) are more likely to recur during 72 months ER positive tumors. What is the overlap between the different groups of miRs?
2. “miR-148b in addition resulted modulated also in ER+/ER- and PR+/- (Figure S2 and S3) “ sentence unclear.
3. Supplementary Table 1: HER2 status of the tumors would be of interest.
4. Figure 1 and 6: How do the survival curves compare to those you would obtain if you were look at ER status or grade?
5. Result section: unclear how mir-148b was localized to intron 1 of COPZ1. Is there evidence for a more widespread transcriptional deregulation of that locus, i.e. are neighbouring genes miRs also affected. Has this region of chromosome 12 been reported to be amplified?

Prof. C. Brisken

## “CURRICULUM VITAE”

**Daniela CIMINO**

**Birth date:** 05/30/1965  
**Birth place:** Torino, Italy  
**Citizenship:** Italian  
**Email:** [daniela.cimino@unito.it](mailto:daniela.cimino@unito.it)  
[daniela.cimino@tin.it](mailto:daniela.cimino@tin.it)

**July 1984:** High School Diploma, Liceo Classico Vittorio Alfieri, Torino.

**October 1998:** University enrolment, Scienze MFN - University of Turin.

**March 2001 - June 2001:** Training on the premises of Pathology Department, University of Turin, G. Bonelli Professor Unit.

**July 2001, the 5th:** Diploma degree in Biological Science, Molecular Cellular advice, University of Turin. Final Report title: "Study Techniques of Apoptosis in primary culture of hepatocytes", Tutor G. Bonelli Professor.

**March 2002, the 12th:** First Degree in Biological Science, University of Turin, grade 110/110 cum laude. First Degree Thesis title: "Gene expression analysis techniques employed to analyze rhCG modulated genes in MCF-7 breast cancer cell line", Tutor M. De Bortoli Professor.

**June 2002, I° Examination Session:** Junior Biologist Qualification, University of Turin, grade 160/200.

**October 2005, the 21th:** Advanced Degree in Biomolecular Sciences, University of Turin, grade 107/110. Advanced Degree Thesis title: "Evaluation of Breast Cancer Aggressiveness Molecular Sources by High Throughput Gene Expression Analysis", Tutor M. De Bortoli Professor.

**December 2010, the 17th:** PhD thesis dissertation, PhD school in Complex System in Medicine and Life Science, University of Turin. PhD Thesis title: "miR-148b is a major coordinator in a Relapse-associated miR signature in Breast Tumors", Supervisor D. Taverna.

### **Research Experiences:**

**09/01/2001 – 21/31/2001:** Contratto di prestazione d'opera stipulato con il Dipartimento di Biologia Animale e dell'Uomo. Argomento: Analisi della regolazione genica da hCG

mediante RT-PCR. Svolto presso: Gynecological Oncology Unit - Istituto per la Ricerca e la Cura del Cancro-Candiolo.

**01/04/2002 - 31/03/2003:** Contratto di collaborazione coordinata e continuativa stipulato con la Fondazione Scientifica Mauriziana-ONLUS. Argomento: *Expression profiles of selected gene clusters in breast tumors as indicators of metastatic potential*. Svolto presso: Unità di Ginecologia Oncologica, Istituto per la Ricerca e la Cura del Cancro-Candiolo.

**01/04/2003 - 31/03/2004:** Contratto di collaborazione coordinata e continuativa stipulato con la Fondazione Scientifica Mauriziana-ONLUS. Argomento: *Expression profiles of selected gene clusters in breast tumors as indicators of metastatic potential*. Svolto presso: Unità di Ginecologia Oncologica, Istituto per la Ricerca e la Cura del Cancro-Candiolo.

**01/04/2004 - 31/03/2005:** Contratto di lavoro a progetto stipulato con la Fondazione Piemontese per la Ricerca sul Cancro-ONLUS. Argomento: Profili di espressione di gruppi selezionati di geni nei tumori mammari come indicatori di potenziale metastatico. Svolto presso: Unità di Ginecologia Oncologica, Istituto per la Ricerca e la Cura del Cancro-Candiolo.

**01/04/2005 - 31/03/2006:** Contratto di lavoro a progetto stipulato con la Fondazione Piemontese per la Ricerca sul Cancro-ONLUS. Argomento: Risposta genomica ad estrogeni ed antiestrogeni nel carcinoma della mammella. Svolto presso: Unità di Ginecologia Oncologica, Istituto per la Ricerca e la Cura del Cancro-Candiolo.

**01/04/2006 - 28/02/2007:** Contratto di lavoro a progetto stipulato con la Fondazione Piemontese per la Ricerca sul Cancro-ONLUS. Argomento: Risposta genomica ad estrogeni ed antiestrogeni nel carcinoma della mammella. Svolto presso: Unità di Ginecologia Oncologica, Istituto per la Ricerca e la Cura del Cancro-Candiolo

**01/03/2007 - 31/10/2007:** Contratto di lavoro a progetto stipulato con la Fondazione Piemontese per la Ricerca sul Cancro-ONLUS. Argomento: Risposta genomica ad estrogeni ed antiestrogeni nel carcinoma della mammella. Svolto presso: Unità di Ginecologia Oncologica, Istituto per la Ricerca e la Cura del Cancro-Candiolo.

**01/11/2007 - 31/10/2009:** Assegno di ricerca, Università degli Studi di Torino, (Sel. A06.140/X) 01/11/2007-31/10/2009 “Profili di espressione genica nel cancro mammario in relazione alla risposta ad estrogeni ed antiestrogeni”.

**01/11/2009 - 30/06/2010:** Borsa di Studio di addestramento alla ricerca su fondi finanziati dalla Regione Piemonte (Sel. n. 12/2009), Ricerca Scientifica Applicata, CIPE2004 dal titolo “Analisi dell’espressione genica di AP-2 durante la trasformazione neoplastica tramite l’utilizzo di microarrays e RNAi”.

**05/07/2010 - now:** Borsa di Studio di addestramento alla ricerca su fondi finanziati / erogati dall Compagnia di San Paolo (Sel. n. 003/2010), nel quadro del progetto dal titolo: "LA RICERCA BIOTECNOLOGICA E L'ATTIVITÀ DI FORMAZIONE DEL NUOVO CENTRO DI BIOTECNOLOGIE MOLECOLARI (CBM) DELL'UNIVERSITÀ DI TORINO". In particolare la Borsa di Studio è destinata al completamento della formazione scientifica nel settore della identificazione e caratterizzazione di microRNAs nel tumore al seno.

## Proceedings

1. Sfiligoi C., **Cimino D.**, Biglia N., Ponzzone R., Berardo F., Sismondi P., De Bortoli M. “Breast Cancer Molecular Profiling: Identification of a Gene Subset Related to Prognosis” 3rd EORTC-NCI International Meeting on Cancer Molecular Markers: From Discovery to Clinical Practice, 18-20 aprile 2004 – Sheraton Brussels Hotel & Towers, Bruxelles, Belgio.
2. Sismondi P., **Cimino D.**, Fuso L., Sfiligoi C., Biglia N., Ponzzone R., De Bortoli M. “A molecular view of breast cancer aggressiveness” The Events of the Year in Gynaecology-Obstetrics, 20-22 Maggio 2004, S. Pietroburgo, Russia.
3. Cardamone M.D., Cordero F., Lazzarato F., Cicatiello G., Scafoglio C., **Cimino D.**, Basile W., Weisz A., Calogero R.A., De Bortoli M. “Bioinformatics and Functional Analysis of ERE-containing Genes” EMBO Conference, Nuclear Receptors: From Chromatin to Disease, 20th anniversary of the cloning of nuclear receptors, 29 settembre – 1 ottobre 2005, Villa Alba, Gardone Riviera, Lago di Garda.
4. **Cimino D.**, Fuso L., Sfiligoi C., Russo G., Sismondi P. and De Bortoli M. “A nucleolar RNA helicase correlates with poor prognosis in breast cancer patients” 6° ISREC Conference on Cancer Research, 11 – 13 ottobre 2006, Losanna, Svizzera.
5. Orso F., Corà D., Penna E., **Cimino D.**, De Bortoli M., Taverna D. and Caselle M. “Identification of new AP-2 $\alpha$  regulated genes: a biological and bioinformatic approach” BITS 2007, 26 – 28 aprile 2007, Napoli.
6. **Cimino D.**, Fuso L., Sfiligoi C., Biglia N., Ponzzone R., Maggiorotto F., Russo G., Weisz A., Taverna D., Sismondi P. and De Bortoli M. “Gene expression profiling of pre-defined sets of neoplastic tissues allows discovery of new

- genes associated with breast cancer progression.” Terzo Seminario nazionale SIBBM, 25 – 27 giugno 2007, Torino.
7. Orso F., Corà D., Penna E., **Cimino D.**, De Bortoli M., Taverna D. and Caselle M. “Identification of new AP-2 $\alpha$  regulated genes: a biological and bioinformatic approach” 15<sup>th</sup> Annual International Conference on Intelligent Systems for Molecular Biology (ISBM) & 6<sup>th</sup> European Conference on Computational Biology (ECCB), 21 – 25 luglio 2007, Vienna, Austria, accettato per presentazione orale.
  8. **Cimino D.**, Fuso L, Sfiligoi C., Russo G., Weisz A., Taverna D., Sismondi P., de Bortoli M. “New genes associated with breast cancer progression identified by gene expression analysis” IX Congresso annuale FISV, 26-29 Settembre 2007, Riva del Garda.
  9. **Cimino D.**, Fuso L, Sfiligoi C., Russo G., Weisz A., Taverna D., Sismondi P., de Bortoli M. “New genes associated with breast cancer progression identified by gene expression analysis” SYSBIOHEALTH Symposium 2007, 16-19 ottobre 2007, UNIVERSITA’ Milano-Bicocca, Milano.
  10. Penna E., **Cimino D.**, Orso F. And Taverna D. “Identification and Characterization of microRNAs Involved in Tumor Progression and Metastasis” Riunione Nazionale Dottorandi, ABCD, Rimini 5-7 giugno 2008
  11. De Pittà C., **Cimino D.**, Solero A., Casara S., Zampini M., Romualdi C., Biglia N., Ponzzone R., Lanfranchi G., De Bortoli M., Sismondi P. and Taverna D. “microRNAs in Breast Tumors” XI Congresso Nazionale SIGU, Genova 23-26 novembre 2008.
  12. **Cimino D.**, De Pittà C., Casara S., Zampini M., Romualdi C., Biglia N., Ponzzone R., Lanfranchi G., De Bortoli M., Sismondi P., Taverna D. “MicroRNA (miR) and cancer progression in Breast Tumors” Messenger RNA 3' ends and Gene Expression EMBO workshop, Oxford UK 16-20 settembre 2009.
  13. Penna E., Orso F., **Cimino D.**, Tenaglia E., De Pittà C., Casara S., Lembo A., Pinatel E., Quaglino E., Osella S., Lanfranchi G., Bernengo M.G., Provero P., Taverna DF. “microRNA-214 promotes melanoma tumor progression” meeting ABCD “Mechanisms of Signal Transduction”, Fiesole (FI) 26-27 marzo 2010.
  14. De Pittà C., **Cimino D.**, Casara S., Zampini M., Romualdi C., Biglia N., Ponzzone R., Lanfranchi G., De Bortoli M., Sismondi P., Taverna D. “microRNA and cancer progression in Breast Tumours” 4th ESF Conference on Functional Genomics and Disease, Dresda, Germania, 14-17 aprile 2010.
  15. **Cimino D.**, De Pittà C., Casara S., Pinatel E., Orso F., Zampini M., Romualdi C., Ponzzone R., Briskin C., Provero P., De Bortoli M., Sismondi P., Lanfranchi G. and Taverna D. ”microRNA and cancer progression in Breast

Tumours” Gordon Conference: Mammary Gland Biology, 06/06/2010 - 06/11/2010, Il Ciocco Hotel and Resort, Lucca (Barga) Italy.

16. **Cimino D.**, De Pittà C., Casara S., Pinatel E., Orso F., Zampini M., Romualdi C., Ponzzone R., Brisken C., Provero P., De Bortoli M., Sismondi P., Lanfranchi G. and Taverna D. ”microRNA and cancer progression in Breast Tumours”. MetaFight Public Workshop, “Unravelling Cancer Cell Invasion and Metastasis”, Turin (Italy), 2-3 December 2010.

## Scientific Publications

1. Sismondi P, Biglia N, Ponzzone R, Fuso L, Scafoglio C, Cicatiello L, Ravo M, Weisz A, **Cimino D**, Altobelli G, Friard O, De Bortoli M. “Influence of estrogens and antiestrogens on the expression of selected hormone-responsive genes.” *Maturitas*. 2007 May 20;57(1):50-5. Epub 2007 Mar 28.
2. Ravo M, Mutarelli M, Ferraro L, Grober OM, Paris O, Tarallo R, Vigilante A, **Cimino D**, De Bortoli M, Nola E, Cicatiello L, Weisz A. “Quantitative expression profiling of highly degraded RNA from formalin-fixed, paraffin-embedded breast tumor biopsies by oligonucleotide microarrays.” *Lab Invest*. 2008 Apr;88(4):430-40. Epub 2008 Feb 25.
3. F. Orso, E. Penna, **D. Cimino**, E. Astanina, F. Maione, D. Valdembri, E. Giraud, G. Serini, P. Sismondi, M. De Bortoli and D. Taverna. “AP-2alpha and AP-2gamma regulate tumor progression via specific genetic programs.” *FASEB J*. 2008 Aug;22(8):2702-14. Epub 2008 Apr 28.
4. **D. Cimino**, L. Fuso, C. Sfiligoi, N. Biglia, R. Ponzzone, F. Maggiorotto, G. Russo, A. Weisz, D. Taverna, P. Sismondi and M. De Bortoli. “Identification of new genes associated with breast cancer progression by gene expression analysis of pre-defined sets of neoplastic tissues.” *Int J Cancer*. 2008 Sep 15;123(6):1327-38.
5. E. Penna, F. Orso, **D. Cimino**, E. Tenaglia, A. Lembo, E. Quaglino, L. Poliseno, S. Osella, C. De Pittà, E. Pinatel, P. Provero, M.G. Bernengo, I. Osman and D. Taverna. “microRNA-214 contributes to melanoma tumor progression through suppression of TFAP2C”. Submitted to *EMBO J.*, under revision.
6. A. Courtin, L. Desreumaux, **D. Cimino**, M. Vilasco, M. De Bortoli, D. Taverna, AM. Faussat, N. Mourra, M. Chaouat, P. Forgez and A. Gompel. “Glucocorticoid receptor activity discriminates between progesterone and

medroxyprogesterone acetate effects in breast cells.". Submitted to Breast Cancer Research and Treatment.

7. **D. Cimino**, C. De Pittà, F. Orso, M. Zampini, E. Pinatel, S. Casara, C. Romualdi, R. Ponzzone, C. Brisken, P. Provero, M. De Bortoli, P. Sismondi, G.Lanfranchi and D. Taverna. "miR-148b is a major coordinator in a Relapse-associated miR signature in Breast Tumors". In preparation.

20 December 2010

Daniela CIMINO